Plasma Wave Electric Fields in the Solar Wind: Initial Results From Helios 1

DONALD A. GURNETT[1]

Max-Planck-Institut für extraterrestrische Physik, 8046 Garching, West Germany

ROGER R. ANDERSON

Department of Physics and Astronomy, University of Iowa, Iowa City, Iowa 52242

Plasma wave measurements provided by Helios 1 show that the electric field intensities in the solar wind are usually very low, much lower than those for comparable measurements near the earth, where particles moving upstream from the bow shock often cause large disturbances in the solar wind. The most commonly occurring plasma wave detected by Helios is a sporadic emission at frequencies from about 1 to 10 kHz, between the electron and ion plasma frequencies. These waves are thought to be ion sound waves which are Doppler-shifted upward in frequency from below the ion plasma frequency. The maximum electric field intensity of these waves is a few hundred microvolts per meter. At higher frequencies, from about 20 to 100 kHz, electron plasma oscillations are detected at frequencies near the local electron plasma frequency. These electron plasma oscillations are more intense, with field strengths sometimes as large as a few millivolts per meter, but occur very infrequently. Both the ion sound waves and the electron plasma oscillations show a tendency to occur at higher frequencies closer to the sun but no pronounced variation in intensity with radial distance from the sun. In four cases, electron plasma oscillations have been found in association with type III radio bursts.

INTRODUCTION

In this paper we survey and analyze the electric field measurements obtained from the University of Iowa plasma wave experiment on the Helios 1 spacecraft. Helios 1, which was launched on December 10, 1974, is in an eccentric solar orbit near the ecliptic plane with initial perihelion and aphelion radial distances of 0.309 and 0.985 AU, respectively. The University of Iowa plasma wave experiment on Helios 1 provides measurements of electric field intensities in the frequency range from 31 Hz to 178 kHz. This frequency range includes most of the characteristic frequencies of the plasma (the electron plasma frequency f_p^-, the ion plasma frequency f_n^+, and the electron gyrofrequency f_g^-) expected in the solar wind from 0.3 to 1.0 AU. The data obtained from this experiment provide the first observations of plasma waves in the region close to the sun ($R \simeq 0.3$ AU) and measurements with greatly improved sensitivity and frequency range in comparison to any previous solar wind plasma wave investigations performed at 1.0 AU.

Plasma waves play a crucial role in most, if not all, plasma interactions which take place in low-density collisionless plasmas. When the mean free path of the particles becomes much larger than the basic scale length of the system, as occurs in the solar wind and the earth's magnetosphere, collisions can no longer provide the mechanism for energy and momentum exchange between the particles. As the system evolves, deviations from thermal equilibrium occur which produce unstable particle distributions. In the region of instability, waves develop which grow to such large amplitudes that they directly affect the distribution function of the interacting particles. These wave-particle interactions usually tend to drive the distribution function toward thermal equilibrium, the waves playing a role similar to collisions in an ordinary fluid.

In the early solar wind models of *Parker* [1958] it was realized that microscopic collisionless interactions must be present to account for the fluidlike properties of the solar wind. The importance of these collisionless interactions was later confirmed in more detail by the two-fluid calculations of *Hartle and Sturrock* [1968], which showed that the solar wind protons must be heated somewhere inside 1 AU to account for the observed proton temperature and velocity at the earth. Because of the low collision frequency in the solar wind this heating must involve wave-particle interactions. Over the past 10 years, numerous theoretical studies have been performed to try to identify the most important and relevant plasma wave instabilities which occur in the solar wind. See, for example, the recent review by *Hollweg* [1975]. Most of these studies have concentrated on various types of low-frequency hydromagnetic (Alfvén) waves and instabilities which occur at frequencies below the ion gyrofrequency. The properties of these low-frequency hydromagnetic waves have now been extensively studied by using satellite-borne magnetometers on interplanetary spacecraft (see, for example, *Coleman* [1966], *Belcher and Davis* [1971], and *Burlaga* [1971]). At higher frequencies, in the range appropriate for comparison with the Helios plasma wave measurements, several types of electrostatic and electromagnetic instabilities have been suggested which may play an important role in controlling the macroscopic structure of the solar wind. *Fredricks* [1969] suggested that electrostatic ion sound waves, driven by currents at discontinuities in the solar wind, could heat the protons in the solar wind by resonant interactions. Substantial proton heating by waves of this type is only expected at radial distances of less than about 0.3 AU. *Forslund* [1970] considered the possible types of two-stream instabilities which could occur because of the skewing of the electron distribution function caused by heat conduction in the solar wind. Four types of instabilities were found which could be driven by electron heat conduction: electromagnetic ion cyclotron, electrostatic ion cyclotron, magnetoacoustic, and ion acoustic. Any of these modes could in principle be unstable in the solar wind at 1 AU.

Schulz and Eviatar [1972] and *Hollweg* [1975] have suggested that these heat conduction driven instabilities may significantly lower the heat conduction in the solar wind, with corresponding modifications of the radial temperature gradient. When streams of energetic electrons are ejected into the solar wind by a solar flare, electron plasma oscillations are expected to be produced by two-stream instabilities at frequencies near the electron plasma frequency. Electron plasma oscillations have received extensive theoretical study because of their presumed relationship to solar radio emissions, particularly type III solar radio bursts [*Ginzburg and Zheleznyakov*, 1958; *Sturrock*, 1961; *Tidman et al.*, 1966; *Smith*, 1974]. These waves are thought to play an important role in controlling the energy spectrum and temporal evolution of the energetic 1- to 100-keV solar flare electrons [*Papadopoulos et al.*, 1974].

Although plasma waves are thought to be of considerable importance in the solar wind, relatively little is known about the types of waves which occur in the solar wind at frequencies above the ion gyrofrequency. Near the earth many measurements of plasma wave electric and magnetic fields have been made in the solar wind with sensitive and reliable instruments. However, in the absence of interplanetary shocks or other large-scale disturbances the proper identification of the waves intrinsic to the solar wind from measurements near the earth is greatly complicated by the disturbing effects of particles arriving from the earth's bow shock and magnetosphere. By very careful investigation of the particle distribution functions to determine the origin of the particles producing an instability, it is possible to identify waves intrinsic to the solar wind. An example of an investigation of this type is given by *Gurnett and Frank* [1975], in which electron plasma oscillations associated with electrons from a solar flare are identified by the Imp 8 spacecraft near the earth. Because of the difficulty of separating out the effects caused by the earth's interaction with the solar wind, few measurements of this type have been made near the earth.

In interplanetary space, far away from the disturbing effects of the earth, the only previous measurements of high-frequency plasma waves ($f \gg f_g^+$) are from the Pioneer 8 and 9 spacecraft [*Scarf et al.*, 1968; *Scarf and Siscoe*, 1971], which provided electric field measurements in the solar wind at radial distances between about 0.75 and 1.0 AU. Since the Pioneer 8 and 9 electric field experiments were relatively insensitive (they used a short telemetry antenna as an electric field sensor), only the most intense plasma waves could be detected. The principal results of the Pioneer 8 and 9 plasma wave experiments were the occasional detection of strong low-frequency ($f \simeq 400$ Hz) electric field turbulence in the solar wind. Several different types of turbulence were identified depending on the detailed temporal variations and correlations with other parameters. Short-duration 'spikes' in the electric field intensity at ~ 400 Hz tended to occur at discontinuities in the magnetic field or plasma parameters (such as at interplanetary shocks) and were closely associated with the occurrence of sudden commencements and geomagnetic disturbances at the earth [*Siscoe et al.*, 1971]. Detailed studies of the electric field intensities during selected storm periods showed a significant variation in the broadband electric field intensity with radial distance from the sun, with maximum broadband intensities of nearly 50 mV m^{-1} (equivalent 100-Hz sine wave response) at 0.75 AU [*Scarf et al.*, 1973]. Longer-duration events, sometimes lasting for one to several days, were also occasionally observed in the broadband electric field measurements with amplitudes of typically 1-10 mV m^{-1} in the 400-Hz channel [*Siscoe et al.*, 1971]. These long-duration events were found to be correlated with regions of enhanced density, such as occur ahead of high-speed streams. Near the earth, electron plasma oscillations associated with the earth's bow shock were detected by Pioneer 8 and 9 [*Scarf et al.*, 1968]; however, comparable plasma oscillations were not observed in interplanetary space away from the effects of the earth [*Scarf et al.*, 1972].

As will be shown, the plasma wave electric field measurements provided by Helios 1 add considerably to the Pioneer 8 and 9 results by providing measurements over a wider range of frequencies and radial distances and with considerably better sensitivity. For most of the types of waves detected by Helios 1 the electric field intensities are below the sensitivity threshold of the Pioneer 8 and 9 instruments, so no direct comparisons can be made. Waves with intensities comparable to the intense low-frequency spikes and long-duration events observed by Pioneer 8 and 9 have not yet been detected by Helios 1.

INSTRUMENT DESCRIPTION

The plasma wave and radio astronomy experiment of Helios 1 consists of a combination of three instruments: a 16-channel spectrum analyzer from the University of Iowa to provide high
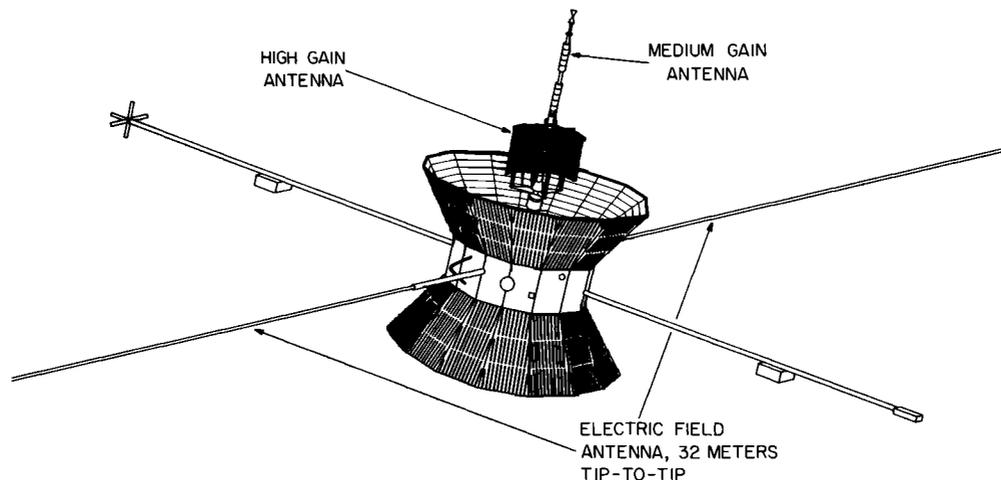
Fig. 1. The geometry of the electric field antenna used for the Helios plasma wave measurements. The spacecraft is spin-stabilized with the medium gain telemetry antenna axis oriented perpendicular to the ecliptic plane.
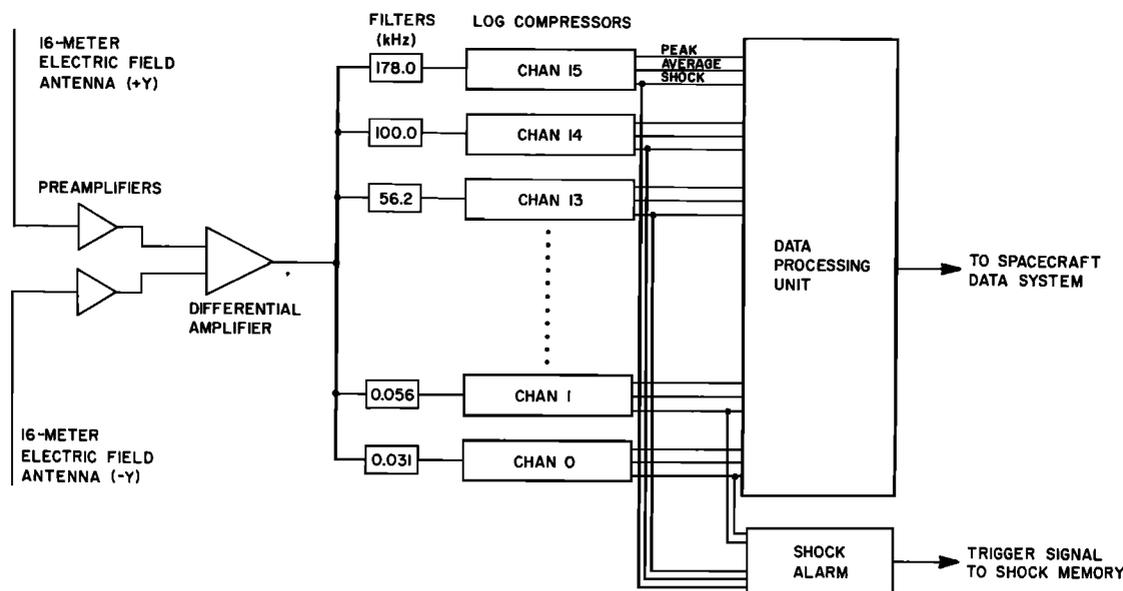
Fig. 2. A block diagram of the University of Iowa plasma wave experiment on Helios. The shock alarm is used to initiate a very rapid sampling rate mode using the spacecraft memory.

time resolution plasma wave measurements in the frequency range from 31 Hz to 178 kHz, a narrow bandwidth spectrum analyzer with 168 frequency steps from the University of Minnesota to provide high frequency resolution plasma wave measurements in the frequency range from 10.4 Hz to 209 kHz, and a 16-channel radiometer from Goddard Space Flight Center to provide solar radio wave measurements in the frequency range from 26.5 kHz to 3.0 MHz. Only results from the University of Iowa instrument are presented in this paper. All three instruments share a single electric dipole antenna with a nominal tip-to-tip length of 32 m, which is extended outward perpendicular to the spacecraft spin axis, as is shown in Figure 1. The spacecraft spin axis is oriented perpendicular to the ecliptic plane, and the nominal spin rate is 1.0 rps.

A block diagram of the University of Iowa plasma wave instrument is shown in Figure 2. This instrument consists of 16 continuously active receiver channels with four frequency channels per decade. The bandwidth of these channels is relatively wide, ±10% for the channels from 31 Hz to 1.78 kHz and ±8% for the channels from 3.11 to 178 kHz. The frequency passbands overlap to provide essentially continuous coverage of all frequencies from about 20 Hz to 200 kHz. The signal from each filter channel is processed by a logarithmic compressor which provides a voltage output proportional to the logarithm of the electric field strength. The dynamic range of the logarithmic compressor is 100 dB. Two types of field strength measurements, called the average and the peak, are made for each channel. The average field strength is the exponentially weighted average (a resistance-capacitance integrator) of the logarithm of the field strength with a time constant of 50 ms for all channels except 56 and 31 Hz, which have time constants of 100 and 200 ms, respectively. The peak field strength is obtained from a peak detector which gives the maximum field strength since the preceding sample. The continuously active channels, with peak detection and overlapping frequency response, assure that any wave which occurs within the frequency and sensitivity range of the instrument will be detected, even very short bursts with durations much shorter than the sampling period. The 16 peak and 16 average field strengths are sampled essentially simultaneously by a data

processing unit which provides analog-to-digital conversion and formating for the spacecraft data system. A wide range of sampling rates is possible, depending in detail on the spacecraft bit rate and telemetry format. The fastest sampling rate in real-time operation provides a complete set of 16 peak and 16 average samples every 1.125 s. Even faster sampling rates, up to 14.2 samples per second for each channel, are possible when a rapid read-in to the spacecraft memory is used. The memory read-in is triggered by a 'shock alarm' circuit (see Figure 2) which responds to the field strength in a preselected channel. A shock alarm signal is generated whenever the field strength exceeds the largest field strength detected since the last memory readout. The memory is organized to store data both immediately before and immediately after the shock alarm signal occurs. The overall function of the shock alarm and memory read-in is to provide very rapid sampling of the electric field spectrum, as well as other magnetic field and plasma data, around the time of maximum field strength.

In-Flight Operation and Near-Earth Observations

Shortly after the launch of Helios 1 it was discovered that one of the two antenna elements which make up the electric dipole antenna did not extend properly and was electrically shorted to the spacecraft structure. The resulting antenna configuration is therefore an electric monopole, the spacecraft body and associated booms acting as a ground plane. Although this is not the intended antenna configuration, the effects of this failure are not particularly serious. Monopole antennas of this type have been successfully used on several previous spacecraft plasma and radio wave experiments [Slysh, 1965; Benediktov et al., 1968; Scarf et al., 1968]. The primary detrimental effects for the Helios 1 experiment are a loss of 6 dB in the electric field sensitivity because of the shorter antenna length and an increase in the noise level of the 178-kHz channel by about 25 dB because of an interference signal conducted into the experiment from the shorted antenna. It was also thought that the reduced common mode rejection caused by the asymmetrical antenna configuration would result in larger interference levels, particularly from the spacecraft solar array. However, comparisons with the Helios
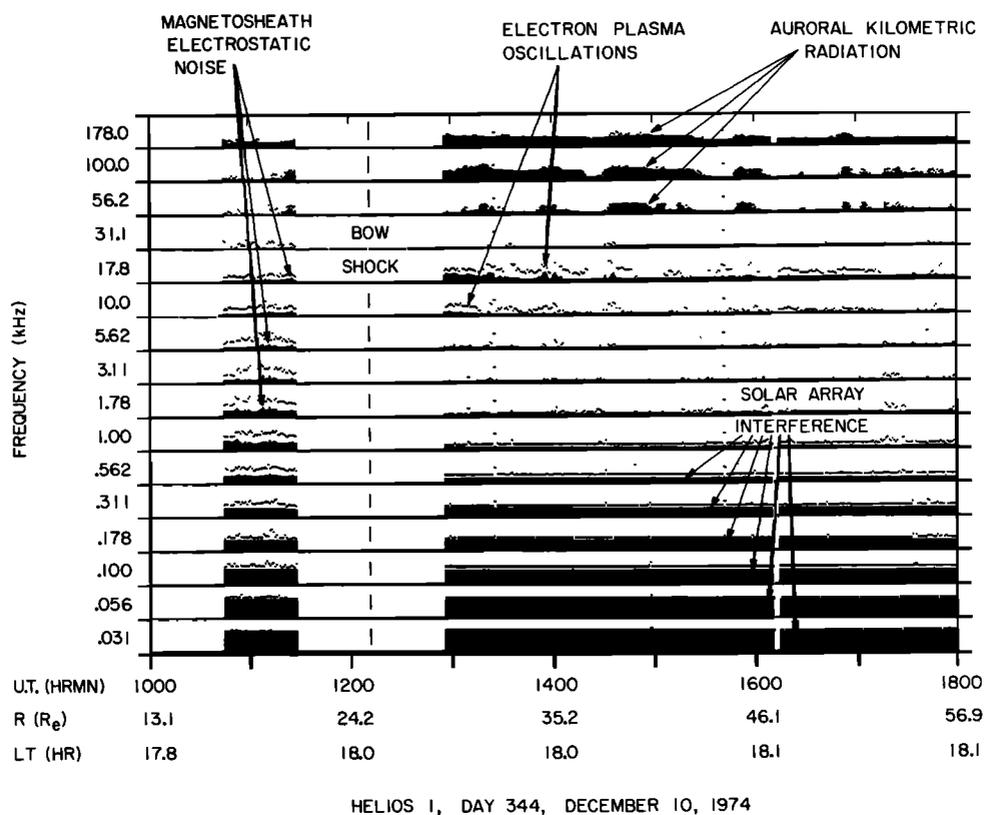
Fig. 3. The electric field intensities detected by Helios 1 during the outbound pass through the bow shock shortly after launch.

2 spacecraft, which was recently launched and for which both antennas extended properly, show that the background noise voltages are essentially the same in all except the 178-kHz channel.

One disadvantage of a monopole antenna is that the effective length cannot be estimated as well as for a dipole antenna because of the complicated geometry of the spacecraft body. To calculate electric field strengths from the Helios 1 data, we assume that the spacecraft body acts as a perfect ground plane, in which case the effective length is one half of the length of the monopole element, or $l_{eff} = 8.0$ m. This assumption is justified mainly on the grounds that the spacecraft body and associated booms have a rather large capacitance to the surrounding plasma which should maintain the spacecraft potential essentially constant with respect to the local plasma potential. At higher frequencies, above the electron plasma frequency where the plasma effects are not important, the effective length is probably somewhat smaller, by about 15–20%, because of the finite size of the ground plane. Because of the large range of electric field strengths encountered in the solar wind, uncertainties of this magnitude are not considered serious. The calculated electric field strengths also rely on the assumption that the wavelengths are longer than the antenna length. In most cases, specific tests based on spin modulation measurements of the antenna pattern and Doppler shift estimates can be performed to verify this assumption.

To demonstrate the operation of the experiment in an environment which has already been extensively investigated, we have analyzed the electric field intensities observed as Helios 1 passes through the region near the earth's bow shock shortly after launch. The electric field intensities in this region are shown in Figure 3 for all 16 channels, from 31 Hz to 178 kHz.

The ordinate for each channel is proportional to the logarithm of the electric field strength, and the interval from the base line of one channel to the base line of the next higher channel represents a range of electric field strengths from about 1 μV m^{-1} to 100 mV m^{-1} for $l_{eff} = 8.0$ m. The peak electric field strengths are indicated by dots, and the average field strengths are indicated by vertical bars (the solid black areas) extending upward from the base line of each channel.

During the pass through the bow shock one of the strongest and most prominent types of noise detected by Helios 1 is a high-frequency (50–500 kHz) radio emission generated in the earth's auroral zones. This noise, which is called terrestrial (or auroral) kilometric radiation [Gurnett, 1974; Kurth et al., 1975], is detectable for several weeks after launch and is clearly evident in the frequency channels above 50 kHz in Figure 3. Auroral kilometric radiation provides a useful source for verifying the effective length of the monopole antenna. During a period of maximum intensity, at a radial distance of 31.1 R_E from the earth (1315 UT), the power flux of the auroral kilometric radiation is found to be 2.98×10^{-15} W m^{-2} at 178 kHz for an effective length of 8.0 m. From a comparison with Figure 5 of Gurnett [1974] it is seen that this power flux is in good quantitative agreement with the typical maximum intensities of auroral kilometric radiation detected by the Imp 6 spacecraft at comparable radial distances from the earth.

Because of the data gap from 1128 to 1255 UT in Figure 3, no plasma wave measurements are available at the time of the actual bow shock crossing. Before the bow shock crossing, during the interval from about 1045 to 1128 UT, a broad spectrum of electric field noise is detected, extending from frequencies below 31 Hz to greater than 56.2 kHz. This noise is characteristic of the intense electrostatic turbulence which is
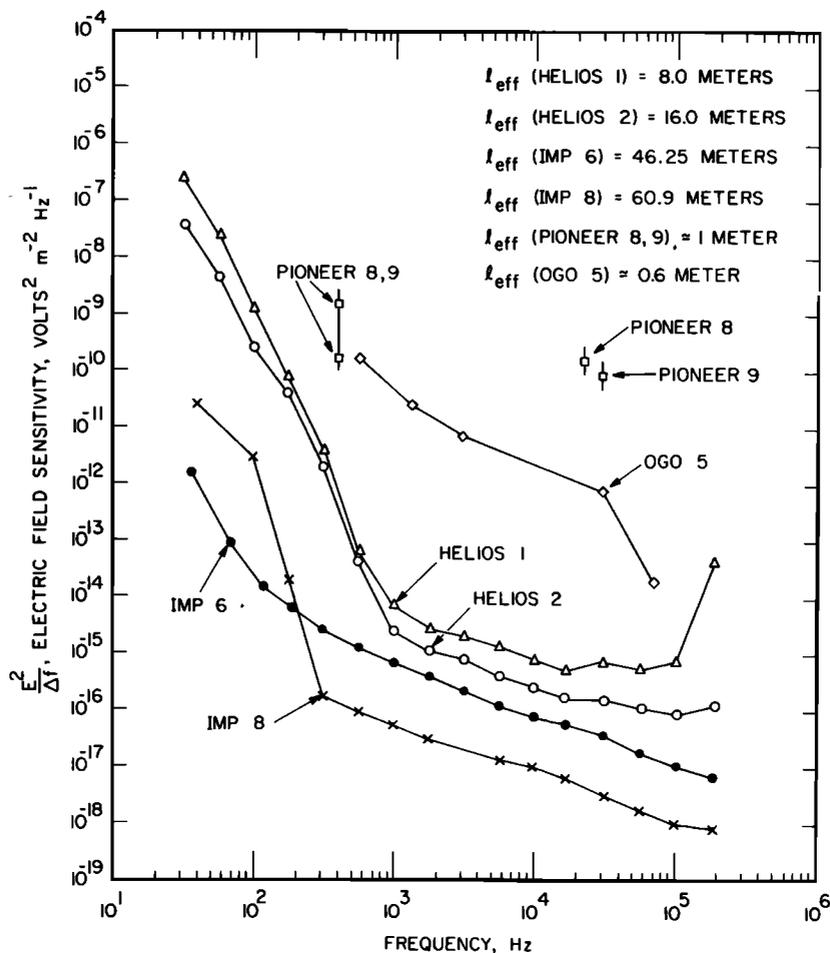
Fig. 4. The threshold electric field sensitivity of Helios 1 and Helios 2 compared to several other plasma wave experiments which have made electric field measurements in the solar wind. The rapid increase in the noise level at low frequencies is caused by interference from the spacecraft solar array.

commonly observed throughout the magnetosheath downstream of the bow shock [Rodriguez and Gurnett, 1975]. After the bow shock crossing, from about 1255 to 1425 UT and in several intervals thereafter, an intense narrow band electric field emission is evident in the 10.0- and 17.8-kHz channels. This narrow band emission consists of electron plasma oscillations of the type discussed by Scarf et al. [1971], excited by electrons streaming into the solar wind from the bow shock. For an effective length of 8.0 m the electric field strength of these plasma oscillations is found to range from about 100 μV m^{-1} to 1 mV m^{-1}, with occasional peaks as large as 3 mV m^{-1}. These field strengths are in good quantitative agreement with similar measurements obtained from the Imp 6 and 8 spacecraft [see Gurnett and Frank, 1975].

In Figure 4 we show the in-flight noise level of the Helios 1 plasma wave experiment (and also Helios 2) and compare these noise levels with several other similar experiments which have made electric field measurements in the solar wind. In each case the noise levels have been calculated by using the effective length determined from strictly geometrical considerations, without regard for errors caused by sheath effects or wavelengths shorter than the antenna. The rapid increase in the noise level of the Helios experiments at low frequencies, below about 1.0 kHz, is caused by interference from the spacecraft solar array. Because of the spacecraft rotation, large voltage transients, as large as 70 V, occur as the solar panels rotate into and out of the sunlight. These voltage transients are

coupled to the antenna through the plasma sheath surrounding the spacecraft and produce strong interference over a very broad range of frequencies. This same type of interference also occurs at low frequencies in the Imp 6 and 8 electric field measurements but is more intense on Helios because of the higher spin rate (1.0 rps) in comparison to the spin rates of Imp 6 and 8 (0.083 and 0.4 rps). The difference in sensitivity between Helios 1 and Helios 2 is caused by the factor of 2 difference in the antenna lengths. The improved sensitivity of the Imp 6 and 8 experiments is mainly due to the longer antennas used on these spacecraft. Since comparisons are to be made later with the Pioneer 8 and 9 electric field measurements, the noise levels of the Pioneer 8 and 9 experiments are also shown in Figure 4, based on the instrument parameters given by Scarf et al. [1968] and Scarf and Siscoe [1971]. The noise levels of the Pioneer experiments assume an effective length of 1.0 m, which, as was pointed out by Scarf et al. [1968], is considered somewhat uncertain because of possible errors introduced by local sheath effects. Also shown for comparison are the noise levels of the Ogo 5 electric field experiment (F. Scarf, personal communication, 1976), which has made electric field measurements in the solar wind [Scarf et al., 1972]. The noise levels of the Ogo 5 7.3- and 14.0-kHz channels are not shown because of the presence of strong spacecraft-generated interference in these channels.

A highly unusual and unexpected interference problem was encountered on Helios 1 when the S band telemetry signal was

U.T.(HRMN) 1400   1600   1800   2000   2200
R (A.U.)   .984   .984   .984   .984   .984

HELIOS I, DAY 346, DECEMBER 12, 1974
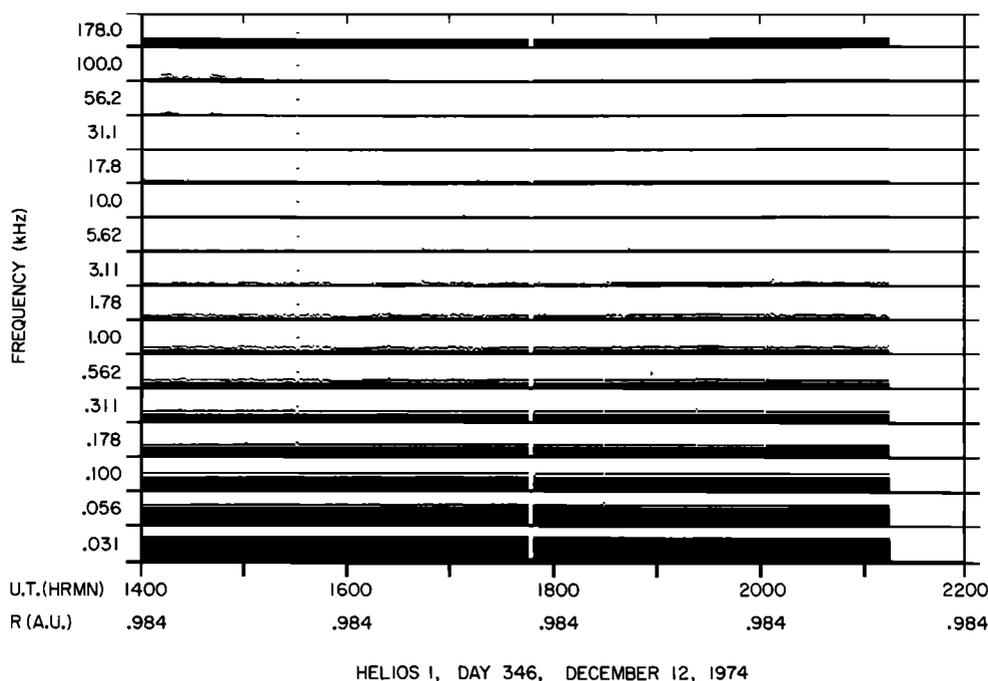
Fig. 5. An example of one of the many 'quiet' periods observed in the Helios 1 plasma wave data.

switched from the medium to high gain telemetry antenna about 10 days after launch. When the telemetry transmitter was switched to the high gain antenna, a very intense broadband interference occurred, with an increase in noise level of nearly 50 dB in some channels. This interference was also accompanied by a number of other dramatic effects indicating a major disturbance in the plasma around the spacecraft, the most notable being a large increase in the $E \simeq 100$ eV electron flux detected by the solar wind plasma experiment (H. Rosen-

Fig. 6. The Helios 1 electric field noise levels at several selected quiet times between launch and first perihelion. These spectrums provide upper limits to the electric field intensities in the solar wind during quiet conditions. The enhanced noise levels near perihelion are believed to be caused by spacecraft-generated interference.

bauer, personal communication, 1976) and a charging of the electric antenna element to -30 to -40 V with respect to the spacecraft structure. Subsequent investigations of these effects have led to the conclusion that the interference and electron heating are caused by a multipacting breakdown of the high gain antenna feed. This breakdown is essentially a transit time resonance for electrons accelerated across the gap in the antenna feed and occurs when the secondary emission coefficient is sufficiently large to cause a rapid buildup of electron density in the gap [Hatch and Williams, 1954, 1958]. Since the resonance condition is highly sensitive to the gap spacing, the antenna feed on Helios 2 was redesigned with a larger gap spacing to eliminate this problem. As a result of this modification, no similar interference effects have yet been observed on Helios 2.

Because of the multipacting problem with the high gain antenna, useful plasma wave data could initially be obtained only by using the medium gain antenna. Since operation with the medium gain antenna resulted in a larger bit rate penalty to the other experiments, this mode of operation was quite limited, usually consisting of only a few 8-hour passes per week. Fortunately, shortly after the first perihelion passage the multipacting interference completely disappeared, and it has not reappeared again except for a short period during the second perihelion passage. The disappearance of the multipacting breakdown is not understood in detail but is generally thought to be caused by modifications of the surface properties (secondary electron emission coefficient) of the high gain antenna feed due to the high temperatures encountered near perihelion.

Since some of the results which will be presented involve the detection of relatively rare plasma wave phenomena, it is important to comment on the total quantity of data which has been analyzed. For this study all of the real-time data obtained from Helios 1 during the first 16 months of in-flight operation, consisting of approximately two and one-half orbits around the sun, have been processed and analyzed in detail. In addition, a survey has been made of the data currently available from Helios 2 during the first 2.5 months of in-flight operation.
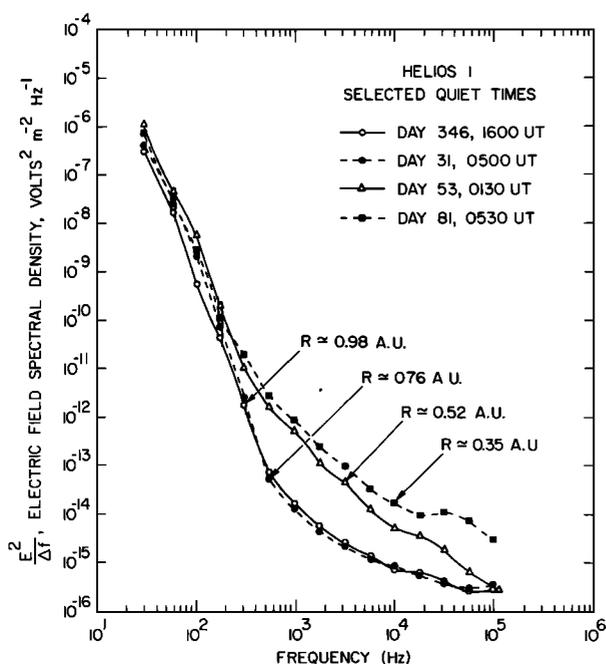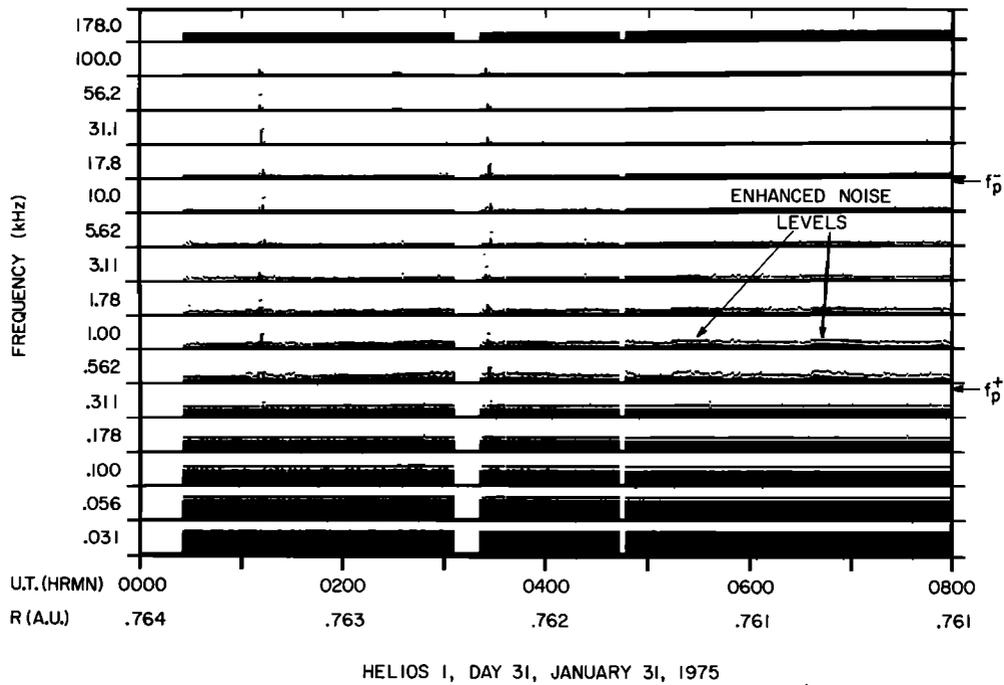
Fig. 7. Another example of a quiet period in which slightly enhanced noise levels are clearly evident in the 562-Hz to 3.11-kHz channels.

Because of the multipacting interference early in the flight of Helios 1 and the reduced telemetry coverage after the first perihelion the overall fraction of the time for which usable plasma wave data are available is only about 30%. This limitation in the available data significantly reduces the detection rate for relatively infrequent events such as type III solar radio bursts and interplanetary shocks. No interplanetary shocks have yet been identified in the Helios plasma wave data, although such events may be identified later when more detailed comparisons are made with the plasma and magnetic field data.

Quiescent Conditions in the Solar Wind

A characteristic feature of the Helios 1 plasma wave data is the almost complete absence of detectable electric fields for a substantial fraction of the time, 50% or more, and for long periods, sometimes lasting several days or longer. This is in striking contrast to measurements in the solar wind near the earth, where moderately intense plasma waves, produced by particles arriving from the bow shock and magnetosphere, are present a large fraction of the time. The electric field intensities during one such quiescent period are shown in Figure 5. Except for some very low intensity waves between about 562 Hz and 3.11 kHz, which will be discussed shortly, all of the electric field channels are near their minimum noise level, as determined by the solar array noise at frequencies below about 1.0 kHz and by the preamplifier noise at frequencies above 1.0 kHz. Comparable quiescent periods are a common feature of the Helios data at all radial distances from 1.0 to 0.3 AU. One notable effect, which was observed on both the first and the second perihelion passage, is a gradual increase in the background noise level with decreasing radial distance from the sun. This radial dependence is illustrated in Figure 6, which shows electric field spectrums selected at four representative radial distances during quiet times. The quiescent noise levels are seen to remain essentially constant from 0.98 to 0.76 AU but then to increase gradually by about 10–15 dB with decreas-

ing radial distance, reaching maximum intensity near perihelion. Although the origin of the increased noise level near perihelion is not known, it is reasonably certain that this noise is not caused by plasma waves. The reason for this conclusion is that the noise intensity displays a pronounced variation with the spacecraft rotation, with a single maximum when the antenna is pointing away from the sun. To be interpreted as an electric field, the spin modulation must have two maximums per rotation. The most likely explanation is that the noise is caused by some type of spacecraft-generated interference which increases in intensity near perihelion. Numerous param-
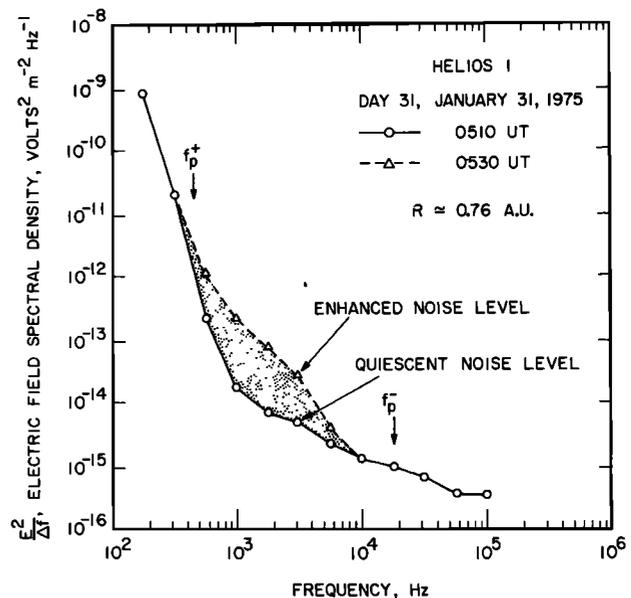
Fig. 8. An electric field spectrum during one of the periods of enhanced noise level evident in Figure 7. The broadband electric field strength of the waves which produce these enhancements is only about $10 \ \mu V \ m^{-1}$.
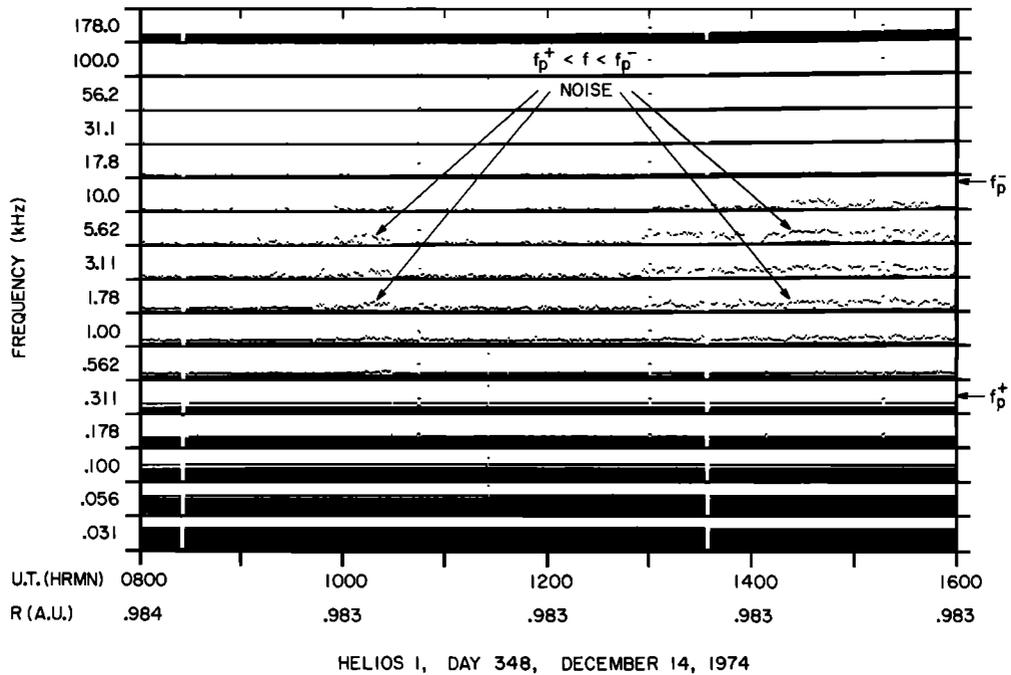
Fig. 9. A more disturbed period during which moderately intense electric fields are detected over a broad range of frequencies between electron and ion plasma frequencies $f_p{}^-$ and $f_p{}^+$. The plasma frequencies are computed from the plasma densities measured simultaneously by the solar wind plasma experiment on Helios.

eters of the spacecraft power system, which could possibly affect the interference levels at high frequencies, vary considerably with radial distance from the sun.

During quiescent periods such as the one in Figure 5 there is often a slight irregular enhancement of the noise level in the 562-Hz to 3.11-kHz channels, suggesting that some very weak plasma waves may be present in this frequency range. An example of the otherwise quiescent interval during which these

low-intensity enhancements are particularly evident is shown in Figure 7. The electric field spectrum during one of the periods of enhanced noise intensity, at 0530 UT, is shown in Figure 8 and is compared with the spectrum at a time of minimum noise level, at 0510 UT. Although it is very difficult to be certain that these periods of enhanced intensity are not caused by spacecraft interference, most of the evidence suggests that these enhancements are caused by plasma waves.
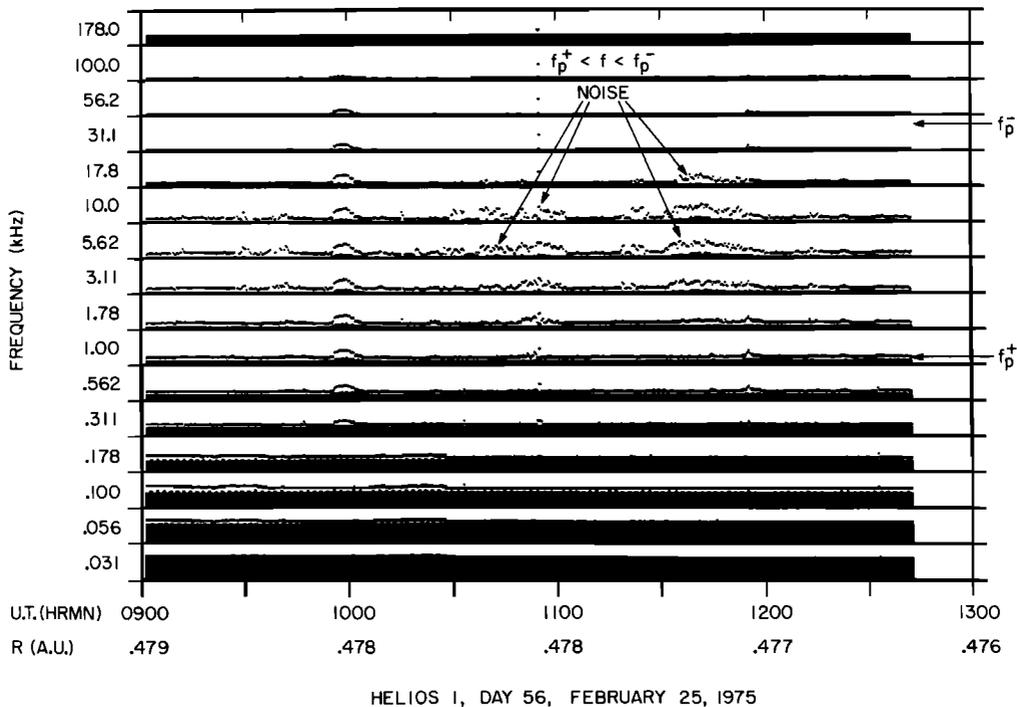
Fig. 10. Another example of the $f_p{}^+ < f < f_p{}^-$ noise, similar to Figure 9 but closer to the sun.

The fact that the enhancements appear in only a limited number of channels indicates that the noise is distinctly different from the multipacting interference and from the interference encountered near perihelion. Also, this same noise is detected even more clearly by Helios 2, which has better electric field sensitivity than Helios 1 and for which no multipacting interference has been detected.

If the very weak irregular enhancements in the 562-Hz to 3.11-kHz channels are due to plasma waves, then the electric field intensity of these waves is very small, the broadband electric field strength being only about 10 μV m^{-1}. Although these waves are very weak, they are apparently present a large fraction of the time, possible 50% or more, because they are almost always detectable, even during quiescent periods such as appear in Figures 5 and 7. Because of the difficulty of clearly resolving these very low intensities, further investigation of these waves will be delayed until more data are available from Helios 2, which has better sensitivity than Helios 1.

Waves Between the Electron and Ion Plasma Frequencies

Occasionally, intervals occur in the Helios 1 plasma wave data in which moderately intense electric field noise is detected in the frequency range from about 1 to 10 kHz. Two examples of this noise are shown in Figures 9 and 10, at radial distances of 0.98 and 0.47 AU, respectively. As will be shown, the frequency range of this noise consistently lies between the local electron and ion plasma frequencies f_p^- and f_p^+. We therefore refer to this noise as $f_p^+ < f < f_p^-$ noise. This terminology is adopted from a strictly observational viewpoint. It should be noted that if sizable Doppler shifts occur, then the actual wave frequencies in the rest frame of the plasma may not, in fact, be directly related to either of these frequencies.

Except for the extremely weak noise enhancements discussed in the previous section, the $f_p^+ < f < f_p^-$ noise is the most commonly occurring type of plasma wave detected by Helios 1. When this noise occurs, it is usually observed with sporadic intensities for periods ranging from a few hours to several days. Such periods of enhanced $f_p^+ < f < f_p^-$ noise intensities usually occur a few times per month. It seems likely that this noise is associated with a corotating feature of the solar wind which recurs for every solar rotation; however, at the present time the available data have not been analyzed in enough depth to establish a definite association. The noise has been detected at essentially all radial distances surveyed by Helios 1.

It is evident in Figures 9 and 10 that the peak intensities of the $f_p^+ < f < f_p^-$ noise are larger than the average intensities by a factor of approximately 20–30 dB. This large ratio of the peak to average field strengths indicates that the noise is very impulsive, consisting of many brief bursts occurring on time scales that are short in comparison to the averaging interval (which is about 1 min for Figure 9 and 30 s for Figure 10). These impulsive temporal variations clearly distinguish this noise from the quiescent noise enhancements, as shown in Figure 7, which have a more nearly constant amplitude. To illustrate the temporal structure of the $f_p^+ < f < f_p^-$ noise, Figure 11 shows a greatly expanded time scale, with 0.28-s resolution, from a shock mode memory read-in which occurred at about 1500 UT during the event in Figure 9. These high time resolution measurements show that the $f_p^+ < f < f_p^-$ noise consists of many short bursts lasting for only a few tenths of a second. Even on this greatly expanded time scale the temporal structure of the individual bursts is sometimes not clearly resolved. Often when an individual burst occurs, it tends to occur simultaneously (within the time resolution available) across a broad range of frequencies.

Typical peak and average frequency spectrums of the $f_p^+ < f < f_p^-$ noise are shown in Figure 12 at times of relatively high intensity selected from the events in Figures 9 and 10. The
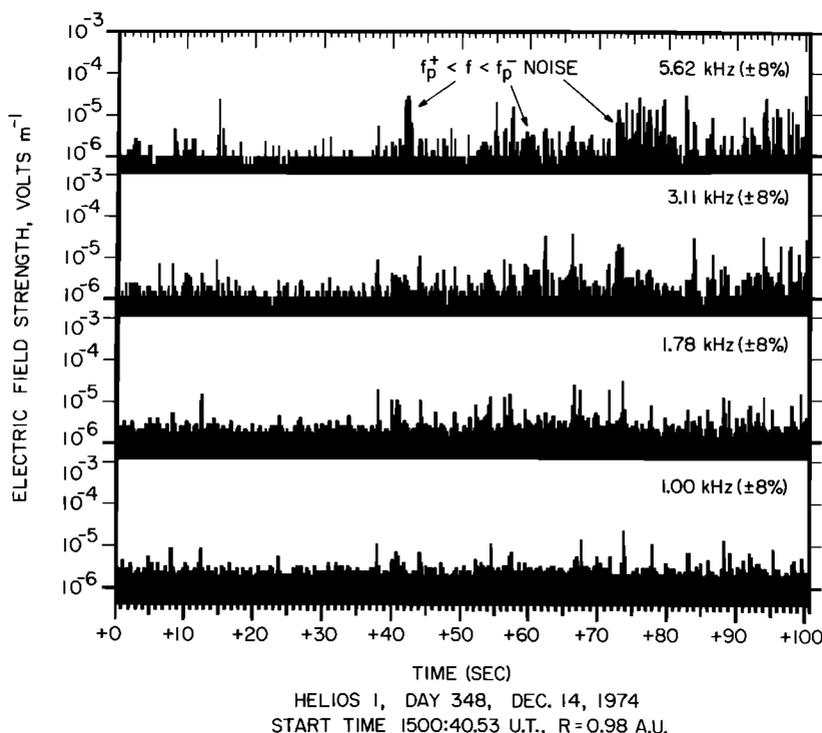
Fig. 11.   High time resolution measurements of the $f_p^+ < f < f_p^-$ noise showing that the noise consists of many short bursts lasting only a few tenths of a second.
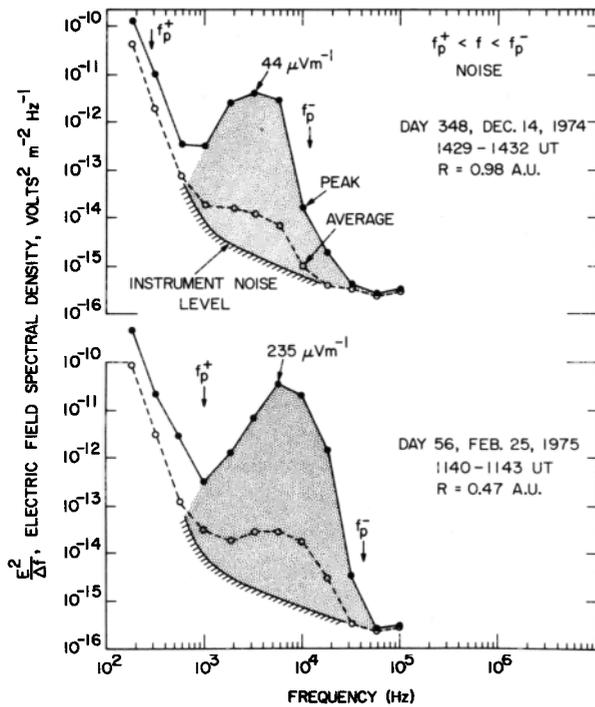
Fig. 12. Selected spectrums of the $f_p^+ < f < f_p^-$ noise showing the shift toward higher frequencies with decreasing radial distance from the sun. Also note the large ratio of the peak to average electric field strength, indicating very impulsive temporal variations.

large ratio between peak and average electric field intensities is clearly evident in these spectrums. Also shown are the electron and ion plasma frequencies as computed from the plasma densities given by the Helios 1 solar wind plasma experiment: f_p^- is computed from the total density of all ions, charge neutrality being assumed, and $f_p^+ = (m_e/m_p)^{1/2}f_p^-$, where m_e and m_p are the electron and proton masses. The spectrums are seen to consist of a single broad maximum between the electron and ion plasma frequencies. By comparing the spectrums for days 348 and 56, at $R = 0.98$ AU and $R = 0.47$ AU, it is seen that the frequency spectrum shifts toward higher frequencies, approximately in proportion to f_p^+ and f_p^-, as the spacecraft comes closer to the sun. Examination of other similar spectrums confirms the tendency evident in Figure 12 for the spectrum to shift toward higher frequencies with decreasing radial distance from the sun. This frequency shift is apparently directly associated with the increase in the electron and ion plasma frequencies as the solar wind density increases near the sun.

The spectrums in Figure 12 also show an increase in the peak electric field strength, from 44 to 235 μV m^{-1}, between day 348 and day 56, the largest field strength occurring closer to the sun. Although this comparison suggests that the electric field intensity of the $f_p^+ < f < f_p^-$ noise may increase with decreasing radial distance from the sun, examination of other similar cases shows that the electric strength variation from event to event is too large to provide any firm conclusion about the radial variation in the electric field intensity. The maximum single-channel electric field strength of the $f_p^+ < f < f_p^-$ noise is typically in the range from about 50 to 300 μV m^{-1} and seldom exceeds 500 μV m^{-1}.

To aid in identifying the plasma wave mode responsible for the $f_p^+ < f < f_p^-$ noise, it is of interest to establish the electric field direction of this noise relative to the magnetic field and solar wind velocity vectors. The electric field direction in the

plane of rotation of the electric antenna can be determined from the spin modulation of the electric field intensities. Because the noise bursts usually occur on a time scale comparable to the time for one rotation (1 s), a statistical analysis must be performed over many events, usually for several hundred spacecraft rotations, to determine an average spin modulation pattern. This procedure is simplified on Helios by the fact that the average (50-ms time constant) field intensity measurements are always sampled in 16 equally spaced angular sectors. However, because of the very low average field strength of the $f_p^+ < f < f_p^-$ noise and the very impulsive intensity variations, simple averaging of the intensity as a function of the sector number does not give a good indication of the spin modulation. The approach used is to compute the frequency of occurrence of field intensities above a given threshold as a function of the threshold and the sector number. The spin modulation is then determined from the contours of constant frequency of occurrence as a function of the sector number. This method of analysis is less sensitive than simple averaging to errors introduced by a few exceptionally intense bursts.

An example of this spin modulation analysis for a $f_p^+ < f < f_p^-$ noise event detected at about 0.98 AU is shown in Figure 13. The accumulation interval for this frequency of occurrence determination is 1 hour. The antenna orientation angle ϕ_{SE}^A is the spacecraft-centered solar ecliptic longitude of the $+Y$ antenna axis, including a correction of 18° to account for the phase shift caused by the 50-ms receiver time constant. The solid and dashed lines give the electric field intensities at frequencies of occurrence of 5 and 10%, respectively. Even with a 1-hour accumulation interval, considerable scatter is still evident in the frequency of occurrence contours. Nevertheless, a consistent modulation pattern is clearly evident with the maximum intensities at about $\phi_{SE}^A \simeq -30°$ and $+150°$. During
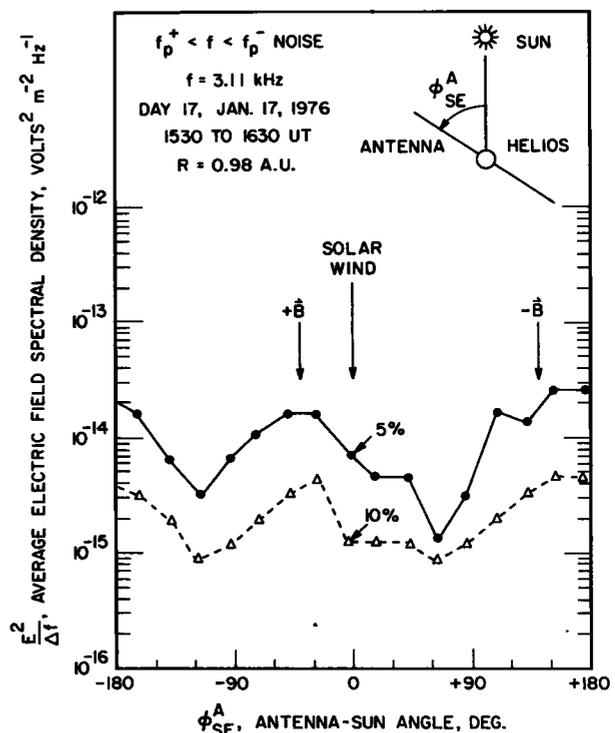
Fig. 13. The angular distribution of electric field intensities for the $f_p^+ < f < f_p^-$ noise. The electric field of this noise is oriented approximately parallel to the direction of the solar wind magnetic field.
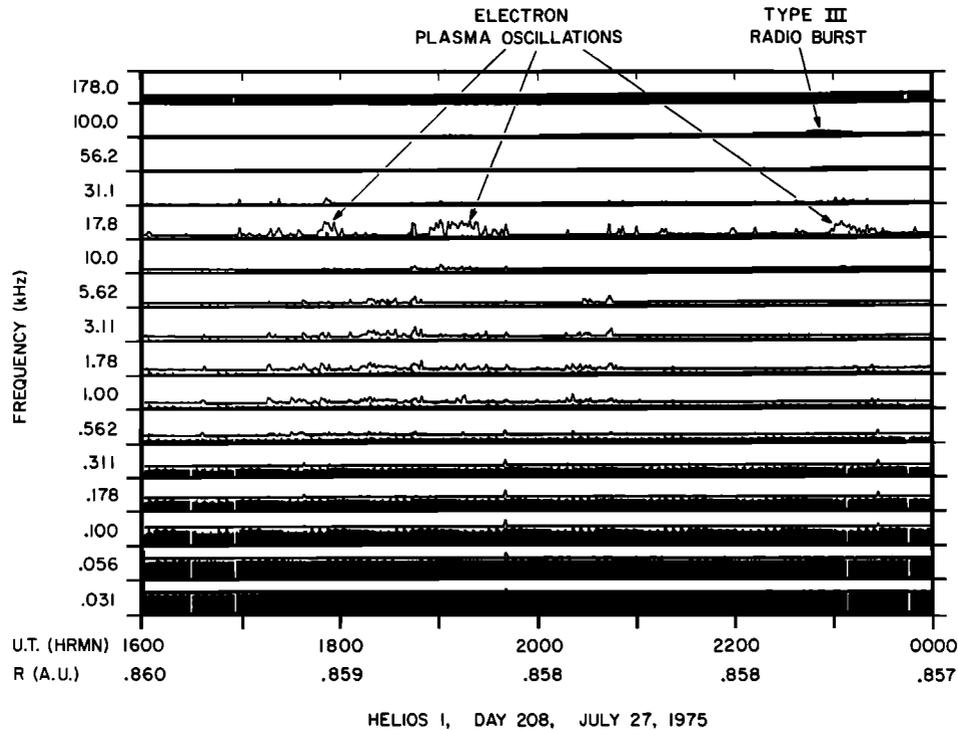
Fig. 14.   Examples of electron plasma oscillations at $f \simeq f_p^-$ detected during a period of enhanced solar flare activity.

this interval the average spacecraft-centered solar ecliptic longitude and latitude of the magnetic field are approximately $\phi_{SE}^B = -40° \pm 10°$ and $\theta_{SE}^B = 0° \pm 20°$, respectively (F. Neubauer, personal communication, 1976). Because the magnetic field is oriented close to the spin plane of the electric antenna, this event provides a good case for determining the electric field orientation relative to the solar wind magnetic field direction. For comparison the magnetic field directions $+\mathbf{B}$ and $-\mathbf{B}$, projected into the plane of rotation of the antenna, are shown in Figure 13. The electric field intensities clearly have a symmetrical distribution with respect to the solar wind magnetic field direction, with the maximum intensity when the antenna axis is aligned parallel to the magnetic field. The sharp nulls in the electric field intensity, by about a factor of 10, indicate that the electric field of the $f_p^+ < f < f_p^-$ noise is very closely aligned along the direction of the solar wind magnetic field, probably to within less than 15°.

Electron Plasma Oscillations

Occasionally, narrow band electric field emissions are detected in the frequency range from about 20 to 100 kHz which are almost certainly caused by electron plasma oscillations at the local electron plasma frequency f_p^-. An example of a period during which electron plasma oscillations are detected by Helios 1 is shown in Figure 14. The identification of these waves as electron plasma oscillations is based on the close similarity of the frequency spectrums and intensities to the electron plasma oscillations observed upstream of the bow shock, as seen in Figure 3. In contrast to the plasma oscillations detected near the earth, which are associated with electrons from the bow shock, the plasma oscillations shown in Figure 14 must be generated by particles of solar origin or by nonthermal particle distributions in the solar wind.

Typically, only one or two brief periods occur per month in which electron plasma oscillations are detected by Helios 1. In most cases the plasma oscillations are observed during a single

isolated interval lasting from a few minutes to about half an hour. The plasma oscillation events which occur on day 208 (in Figure 14) and also continue to day 209 (not shown) represent an exceptionally active period with respect to the occurrence of electron plasma oscillations. This period corresponds to one of the few periods of substantial solar flare activity detected by . Helios 1 during the first year of in-flight operation. On the basis of the previous association of electron plasma oscillations with low-energy (few keV) electrons ejected by a solar flare [*Gurnett and Frank*, 1975] it seems likely that the electron plasma oscillations detected during this period are associated with electrons from this flare activity. Preliminary comparisons with the data from the energetic particle and plasma experiments on Helios 1 (E. Keppler and H. Rosenbauer, personal communication, 1976) confirm that low-energy (1-20 keV) electrons of solar origin are present during this period. The type III radio burst associated with one of these flares is clearly evident in the 100-kHz channel of Figure 14, starting at about 2243 UT. This type III radio burst and others detected by Helios are discussed in the next section.

The electric field spectrum of the electron plasma oscillation detected on day 208, at a time of relatively high intensity, is shown in the top panel of Figure 15. Also shown are the spectrums for two other examples of electron plasma oscillations detected at closer radial distances to the sun. For comparison and confirmation of the identification of these waves as electron plasma oscillations, the local electron plasma frequencies determined from the solar wind plasma experiment are also given in Figure 15. The close correspondence between the emission frequency and the local electron plasma frequency is clearly evident. The spectrums in Figure 15 also show the expected increase in the electron plasma frequency as the solar wind density increases closer to the sun. This tendency, for increasing frequencies closer to the sun, is a general characteristic of all of the electron plasma oscillations detected by Helios 1.
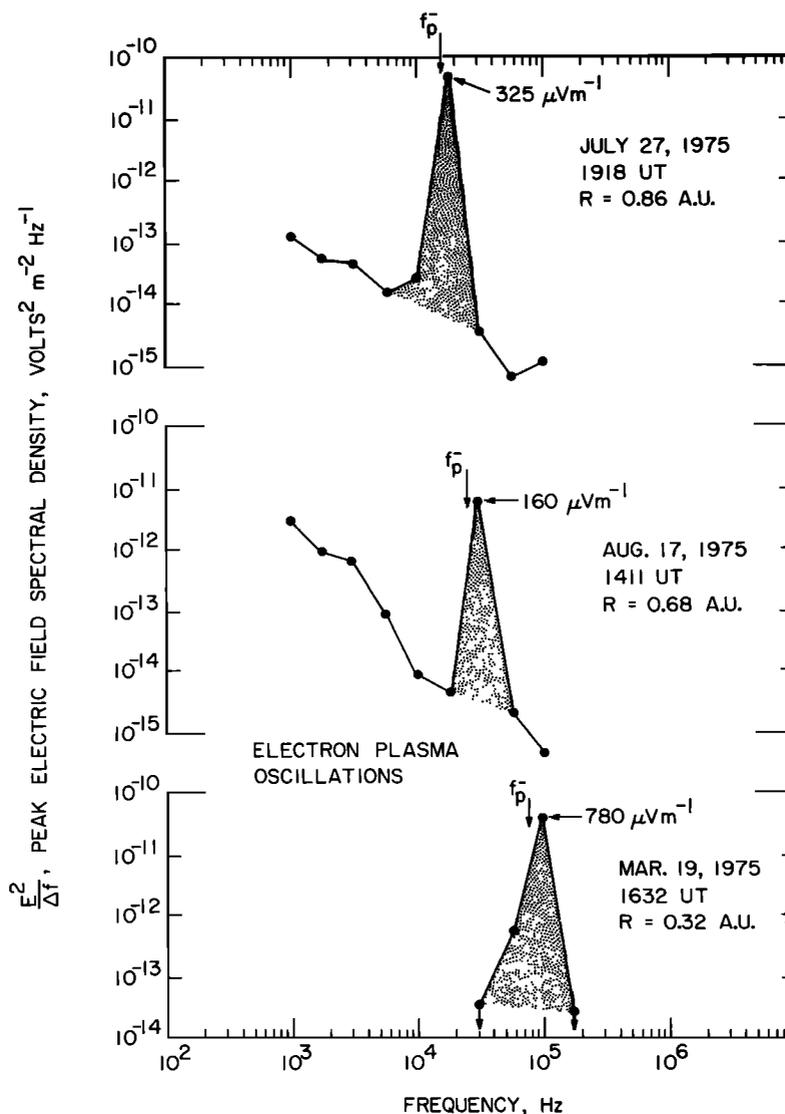
Fig. 15. Selected spectrums of electron plasma oscillations showing the tendency for increasing frequency with decreasing radial distance from the sun. The frequency of the plasma oscillations is in good agreement with the electron plasma frequency f_p determined from the solar wind plasma experiment.

As can be seen from Figure 14, the peak electric field intensities of the electron plasma oscillations are considerably larger than the average field intensities, which remain near the receiver noise level during the entire event. The large ratio of the peak to average field strengths indicates that the electron plasma oscillations, like the $f_p^+ < f < f_p^-$ noise, consist of many brief bursts with durations that are short in comparison to the averaging interval. The temporal structure of a typical burst of electron plasma oscillations is illustrated in Figure 16, which shows a greatly expanded time scale for a series of plasma oscillation bursts detected during a shock mode memory read-in. The rise and decay times of the individual bursts are clearly resolved in these data and are typically in the range from about 0.25 to 1.0 s. In this case the durations of the bursts are only a few seconds. Occasionally, much longer bursts are observed lasting as long as several minutes. When multiple bursts occur, a moderately well defined upper limit to the field strength is often evident (as is true for the first three bursts in Figure 16) and is an indication that some nonlinear effect saturates the instability. The saturation level is usually in the range from about 100 to 500 μV m^{-1}, although occasionally,

larger field strengths do occur, as will be discussed in the next section. Electron plasma oscillations with field strengths exceeding 1 mV m^{-1} are extremely rare. Because of the limited number of events available and the large variation in the intensity from event to event it is not known for certain whether the electric field strength has a significant variation with radial distance from the sun. Some of the most intense events have been observed at radial distances near the sun, as is shown in Figure 15.

As is true for the $f_p^+ < f < f_p^-$ noise, the electric field orientation of electron plasma oscillations can be determined from spin modulation measurements. Because long-duration bursts sometimes occur with nearly constant (saturated) intensities, the spin modulation pattern can be determined very easily in these cases. Figure 17 shows the spin modulation observed during a single rotation for an unusually long (2 min) burst of plasma oscillations detected by Helios 1 near perihelion ($R = 0.332$ AU). During this event the solar wind magnetic field is oriented near the spin plane of the antenna; $\phi_{SE}^B = -15° \pm 3°$, and $\theta_{SE}^B = 19° \pm 1°$ (F. Neubauer, personal communication, 1976) in a direction favorable for determining
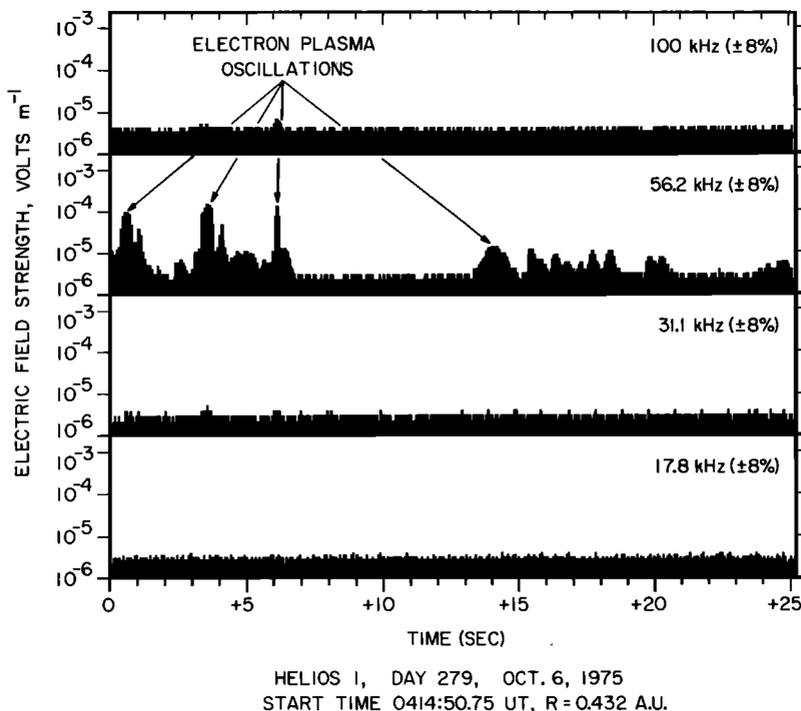
Fig. 16. High time resolution measurements showing several bursts of electron plasma oscillations with durations of only a few seconds. Note the nearly constant saturation amplitude of the first three bursts.

the electric field orientation relative to the magnetic field direction. As can be seen from Figure 17, the maximum electric field intensity occurs when the antenna axis is parallel to the magnetic field. The sharp nulls when the antenna axis is perpendicular to the magnetic field indicate that the electric field of the electron plasma oscillations is very closely aligned along the direction of the solar wind magnetic field, probably to within less than 20°.

trons as they propagate outward from the sun. If the type III radio emission is caused by the conversion of electron plasma oscillations to electromagnetic radiation at $2f_p^-$, as is widely believed, then the onset of the plasma oscillations at the local electron plasma frequency f_p^- should occur essentially simultaneously with the onset of the type III radio emission at $2f_p^-$ and should last for an interval comparable to the duration of

TYPE III SOLAR RADIO BURSTS

One of our primary objectives in studying type III solar radio bursts is to determine whether electron plasma oscillations are involved in the generation of these radio emissions, as has been suggested for many years. In all of the data currently available a total of 18 type III solar radio bursts have been detected by Helios 1 and 2. Of these 18 type III radio bursts, 4 show clear evidence of electron plasma oscillations which could possibly be associated with the radio emission. Two of these events, shown in Figures 18 and 19, occur in association with the solar flare activity on days 208 and 209 (July 27 and 28), 1975, discussed in the previous section, and the second two events, shown in Figures 20 and 21, occur in association with the solar flare activity on day 92 (April 1), 1976.

Before detailed discussion of these events it is useful to consider the ideal 'signature' to be expected if electron plasma oscillations are involved in the generation of type III radio emissions. As is well known, type III radio bursts are produced by electrons ejected into the solar wind by a solar flare. At low frequencies (≤ 1 MHz), considerable evidence exists showing that the type III radio emissions occur at the harmonic $2f_p^-$ of the local electron plasma frequency [Fainberg et al., 1972; Haddock and Alvarez, 1973; Kaiser, 1975]. The characteristic frequency-time dispersion of a type III radio burst, decreasing in frequency with increasing time, is caused by the decreasing electron plasma frequency encountered by the solar flare elec-

Fig. 17. Spin modulation measurements of electron plasma oscillations showing that the electric field of these waves is oriented nearly parallel to the solar wind magnetic field.
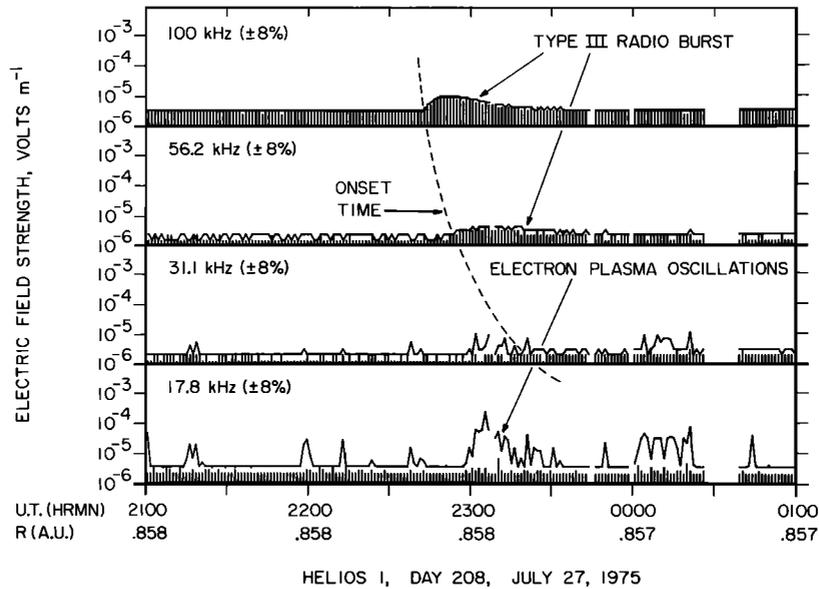
Fig. 18. A type III radio burst which is possibly associated with the electron plasma oscillations detected in the 17.8-kHz channel from about 2257 to 2335 UT. In this case the onset of the electron plasma oscillations at $f_p^- \simeq 20$ kHz is in good agreement with the estimated onset time of the type III radio emission (dashed line) at $2f_p^- \simeq 40$ kHz.

the type III burst at this frequency. Electron plasma oscillations are not expected to be observed for all type III bursts, since the spacecraft must be within the source region to detect the locally generated plasma oscillations.

From the standpoint of the expected plasma wave signature the event on day 208 in Figure 18 represents an excellent example of the expected relationship between electron plasma oscillations and type III radio emission. The onset time of the X ray flare associated with this event is 2232 UT, as determined from the soft X ray detector on Helios 1 (J. Trainor, personal communication, 1976). The type III radio emission produced by the electrons from this flare is first detected in the 100-kHz channel at 2243 UT and subsequently in the 56.2- and 31.1-kHz channels at 2251 and 2313 UT. The approximate

onset times are indicated by the smooth dashed curve in Figure 18. Starting at about 2257 UT, a pronounced burst of electron plasma oscillations occurs in the 17.8-kHz channel, lasting for about half an hour. At the time of maximum intensity the peak electric field strength of these plasma oscillations is about 223 μV m^{-1}. Since the plasma oscillations are detected in the 31.1-kHz channel but not in the 10.0-kHz channel, the electron plasma frequency must be slightly greater than 17.8 kHz, probably about 20 kHz. From the dashed curve in Figure 18 the onset time of the type III radio emission at $2f_p^- \simeq 40$ kHz is estimated to be about 2254 UT, coincident within a few minutes with the onset time of the electron plasma oscillations at $f_p^- \simeq 20$ kHz. By using the 56.2-kHz channel as a guide the duration of the type III radio emission at $2f_p^- \simeq 40$ kHz is esti-
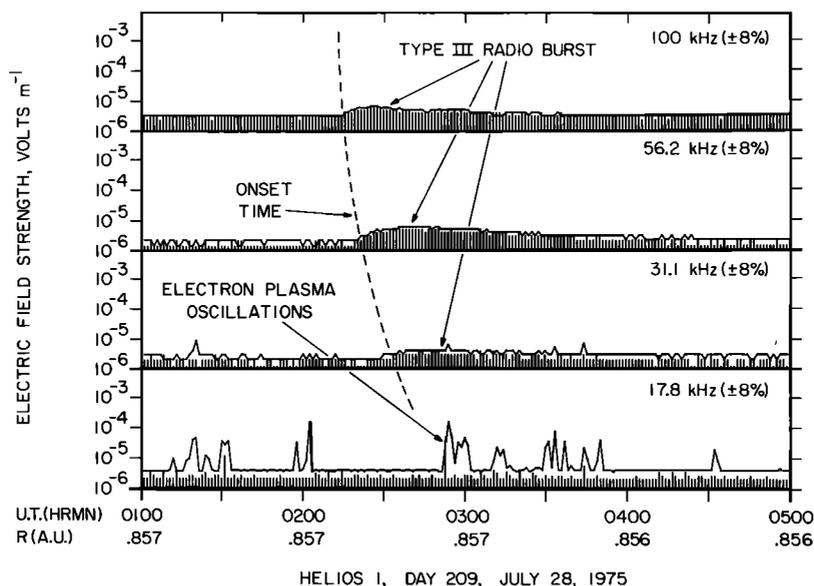
Fig. 19. A type III radio burst and associated electron plasma oscillations occurring a few hours after the event in Figure 18. In this case the onset time of the plasma oscillations is not in good agreement with the onset time of the radio emission at $2f_p^-$. However, the plasma oscillations do occur during the period when a significant level of radio emission is being detected at $2f_p^-$.

mated to be about 35 min, which is comparable to the duration of the electron plasma oscillations. These comparisons are all in excellent agreement with the signature expected for electron plasma oscillations associated with a type III radio burst.

About 3.5 hours after the event in Figure 18, another type III radio burst occurred with electron plasma oscillations. This event is shown in Figure 19. The electron plasma oscillations in this case consist of numerous sporadic bursts lasting for about 1 hour, from 0252 to 0352 UT, with a maximum electric field strength of about 187 μV m^{-1}. In comparison with the event in Figure 18 this event does not fit the ideal signature as well, since the onset time of the plasma oscillations at $f_p^- \simeq$ 17.8 kHz does not agree with the onset time of the radio emission at $2f_p^- \simeq$ 35.6 kHz. Nevertheless, the plasma oscillations do occur within the interval where substantial radio emission is being detected at $2f_p^-$.

By far the best example found to date of electron plasma oscillations associated with a type III radio burst is shown in Figure 20. This event, which occurred on day 92 (April 1), 1976, took place during a period of exceptional solar flare activity from day 83 to day 93, 1976. During this period a total of 11 separate type III radio bursts were detected by Helios 1 and 2. The type III event in Figure 20 is outstanding in that a very intense burst of plasma oscillations, with a maximum electric field strength of 5.26 mV m^{-1}, occurred during the radio burst. These electron plasma oscillations are the most intense ever detected by Helios and are much more intense than the typical electron plasma oscillation events discussed in the previous section. Although the onset of the plasma oscillations occurs somewhat later than the onset of the radiation at $2f_p^-$, the temporal correspondence is so good in this case that there can be essentially no doubt that the radio emission and plasma oscillations are closely associated. Preliminary comparisons with the data from the energetic particle and plasma experiments on Helios (E. Keppler and H. Rosenbauer, personal communication, 1976) confirm that intense fluxes of low-energy (1–20 keV) electrons of solar origin are present during this event. About 4 hours after the event in

Figure 20, another type III radio burst occurred in which correspondingly intense electron plasma oscillations are observed. This event is shown in Figure 21. The electron plasma oscillations in this case are of much shorter duration than those in the event in Figure 20, consisting of only a few brief bursts, but are again unusually intense. The maximum electric field intensity of the plasma oscillations in this case is 2.35 mV m^{-1}.

Considered together, these four events provide substantial evidence confirming that electron plasma oscillations are associated with type III radio bursts. The events in Figures 20 and 21, with plasma oscillation intensities much larger than those in any of the other available data, provide particularly strong evidence of this association. The case is not quite as strong for the more moderate intensity ($\sim$200 μV m^{-1}) plasma oscillations observed during the events in Figures 18 and 19. One obvious interpretational difficulty is that comparable moderate intensity electron plasma oscillations often occur for which no type III radio emission can be detected. Several such cases are evident in Figure 14. Even though the absence of a one-to-one correspondence raises a question of interpretation, it does not conclusively prove that such moderate intensity plasma oscillations cannot in some cases be associated with the type III radio emission. For example, in cases where no radio emission is detected, it is possible that these plasma oscillations are essentially a localized instability occurring in a much smaller volume than the plasma oscillations associated with a type III radio burst. Direction-finding measurements show that the type III source is very large at low frequencies, subtending half angles as large as 45°–60° as viewed from the sun [Baumback et al., 1977].

SUMMARY AND DISCUSSION

The Helios 1 plasma wave measurements show that the electric field intensities in the solar wind are often very low, much lower than those for comparable plasma wave measurements near the earth. During the quiet periods which occur in the Helios 1 plasma wave data the only plasma wave activity
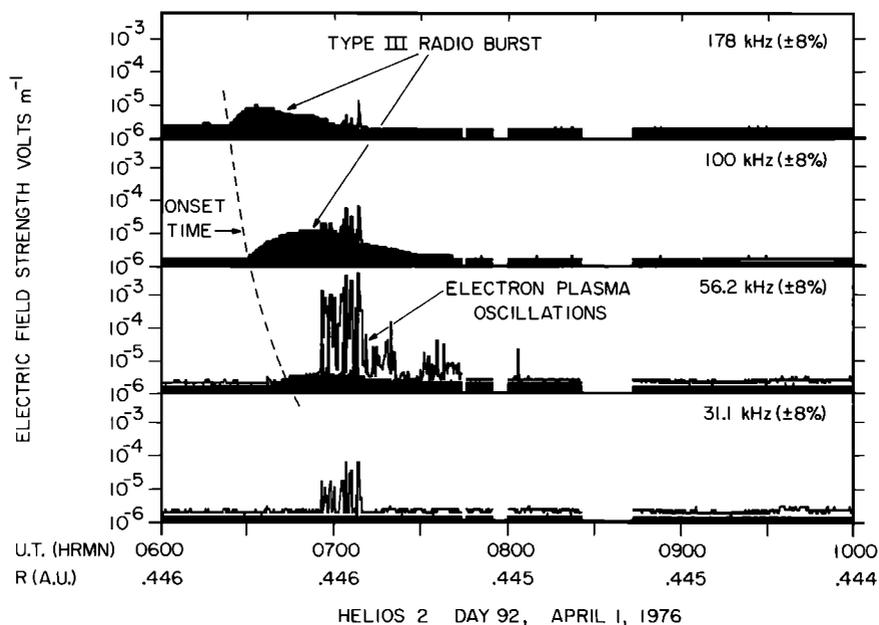
Fig. 20   A type III radio event occurring in association with very intense electron plasma oscillations at $f_p^- \simeq$ 56.2 kHz. The maximum intensity of the plasma oscillations in this case is 5.26 mV m^{-1}. These are the most intense electron plasma oscillations observed to date with the Helios plasma wave experiment.
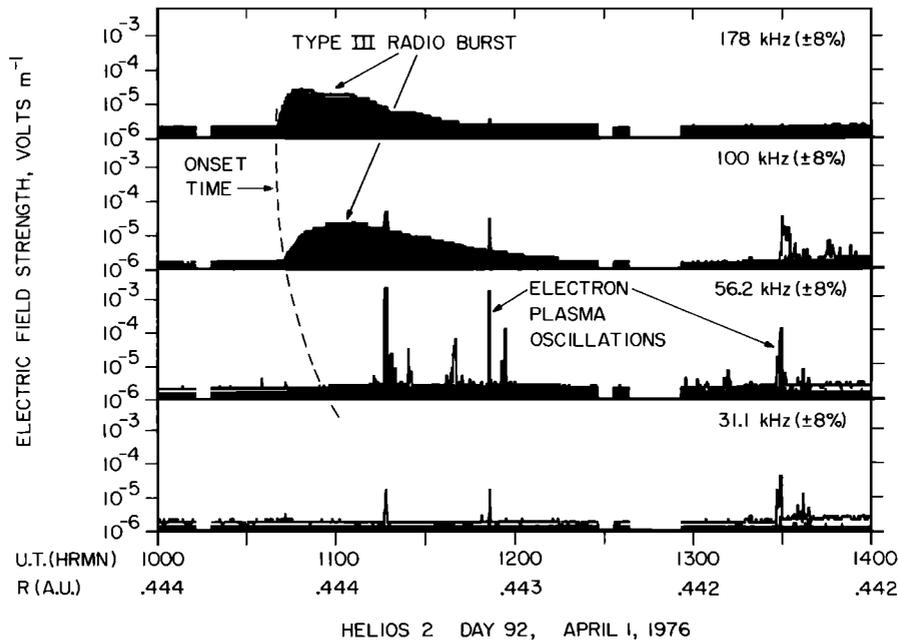
Fig. 21. A type III radio burst and associated electron plasma oscillations occurring a few hours after the event in Figure 20. The maximum intensity of the plasma oscillations in this case is 2.35 mV m^{-1}.

which can be detected is a slight enhancement of the noise levels in the frequency range from about 500 Hz to 3.0 kHz. The broadband electric field strength of these quiet time enhancements is very small, only about 10 μV m^{-1}. During more disturbed periods the most commonly observed plasma wave is a sporadic emission at frequencies between the electron and ion plasma frequencies, typically from about 1 to 10 kHz. These waves are referred to as $f_p^+ < f < f_p^-$ noise. The frequency spectrum of the $f_p^+ < f < f_p^-$ noise shows a systematic variation with radial distance from the sun, shifting toward higher frequencies closer to the sun. The electric field strength of this noise is very impulsive, consisting of many brief bursts lasting for only a few seconds or less with peak single-channel electric field strengths of a few hundred microvolts per meter. No pronounced variation in the electric field strength of this noise is evident with radial distance from the sun. Spin modulation measurements show that the electric field of this noise is closely aligned along the direction of the solar wind magnetic field. At higher frequencies, from about 20 to 100 kHz, narrow band electron plasma oscillations are occasionally detected at frequencies near the local electron plasma frequency. The electron plasma oscillations are more intense than the $f_p^+ < f < f_p^-$ noise, sometimes with electric field strengths as large as a few millivolts per meter, but occur very infrequently. The electric field of the electron plasma oscillations is usually very impulsive and is aligned approximately parallel to the direction of the solar wind magnetic field. The frequency of the electron plasma oscillations closely tracks the local electron plasma frequency as determined by the solar wind plasma experiment and shows a clear systematic variation with radial distance from the sun, increasing in frequency closer to the sun. In all of the available data a total of 18 type III radio bursts have been detected by Helios 1 and 2. Of these, four have simultaneously occurring electron plasma oscillations associated with the type III radio emission. In one of these cases the electron plasma oscillations are unusually intense, with a maximum electric field strength of about 5.26 μV m^{-1}.

In examining the origin of the various types of plasma waves

detected by Helios 1 many interpretational questions must be considered. For the electron plasma oscillations the close tracking of the emission frequency with the local electron plasma frequency and the alignment of the electric field parallel to the solar wind magnetic field strongly support the identification of these waves as electron plasma oscillations. The electric field orientation specifically shows that these waves cannot be associated with the upper hybrid resonance, since waves associated with this resonance would have an electric field orientation perpendicular to the local magnetic field [Stix, 1962]. The basic two-stream instability responsible for the generation of electron plasma oscillations is well known and has been confirmed in some detail by Gurnett and Frank [1975]. The principal questions that remain concern the details of the double-peaked electron distribution function required to produce these waves and the origin of the streaming electrons causing the instability. In some cases, for example, in the event analyzed by Gurnett and Frank [1975] and the events in Figures 18-20 of this paper, it seems reasonably certain that the streaming electrons originate from solar flare activity at the sun. However, other cases occur in the Helios 1 data for which no specific solar flare activity is known to occur, and in these cases the streaming electrons may originate from local acceleration processes in the solar wind. Further studies and comparisons with the plasma measurements are needed to understand fully the conditions and circumstances which lead to the generation of electron plasma oscillations in the solar wind. Since electron plasma oscillations occur very infrequently, it seems unlikely that these waves play a significant role in the steady state properties of the solar wind. These waves may, however, play an important role in thermalizing the low-energy electron streams which sometimes occur in the solar wind. It is also of interest to comment on the very impulsive temporal variations frequently observed for the plasma oscillations detected by Helios. Although the origin of these amplitude fluctuations is not known, it is suggestive, particularly for the very intense events such as occur in Figure 20, that these impulsive variations may be related to a parametric

instability, such as the oscillating two-stream instability proposed by *Papadopoulos et al.* [1974] to stabilize electron streams from solar flares.

The proper identification of the plasma wave mode responsible for the $f_p^+ < f < f_p^-$ noise is more difficult. This noise almost certainly consists of electrostatic waves, since no comparable magnetic field noise has ever been detected in the solar wind. As was mentioned earlier, even though this noise occurs at frequencies between electron and proton plasma frequencies, it is not immediately certain that the noise has any direct relationship to either of these frequencies because of the large Doppler shifts which can occur in the solar wind. If the Doppler shifts are small, $\Delta f/f \ll 1$, the most obvious plasma wave mode which could be associated with this noise is the Buneman mode [*Buneman*, 1958] at $f_B \simeq (m^-/m^+)^{1/3} f_p^-$. However, for the typical solar wind parameters $T_e = (2-6)T_p$ the Buneman mode is not considered a very likely possibility for explaining this noise, since this mode has a higher instability threshold than the ion sound wave and requires a large electron drift velocity in relation to the ions to drive the instability. Although such large drift velocities may occur at discontinuities in the solar wind, it seems unlikely that this instability could occur over the large spatial regions for which the $f_p^+ < f < f_p^-$ noise is observed.

If the Doppler shifts are large, the most likely possibility for explaining the $f_p^+ < f < f_p^-$ noise is thought to be ion sound waves at $f \simeq f_p^+$ which are Doppler-shifted to frequencies above f_p^+ (requires wave vectors $\mathbf{K}$ directed away from the sun). The possible occurrence of an ion sound wave instability in the solar wind has been previously suggested and discussed by *Forslund* [1970]. Because ion sound waves have relatively short wavelengths, the Doppler shift caused by the motion of the solar wind is large in comparison to the wave frequency of $\sim f_p^+$ in the rest frame of the plasma. The frequency detected in the spacecraft frame of reference is approximately

$$f' = f_p^+ + (V/\lambda) \cos \theta_{KV}$$

where V is the solar wind velocity, λ is the wavelength, and θ_{KV} is the angle between $\mathbf{K}$ and $\mathbf{V}$. Since θ_{KV} is typically not near $\pi/2$, the upper cutoff frequency of the observed frequency spectrum is mainly determined by the minimum wavelength ($f_{max} = V/\lambda_{min}$). The minimum wavelength is controlled by the onset of strong Landau damping and is approximately $\lambda_{min} = 2\pi\lambda_D$ where λ_D is the Debye length. For typical solar wind temperatures and densities at 1.0 AU, $T = 1.0 \times 10^5$ °K, and $n = 5$ cm^{-3}, the minimum wavelength is approximately $\lambda_{min} = 61$ m. For a solar wind velocity of 400 km s^{-1} the corresponding f_{max} is 6.5 kHz, which is in good agreement with the observed upper cutoff frequency of the $f_p^+ < f < f_p^-$ noise at 1.0 AU (compare with Figure 12). The increase in the upper cutoff frequency with decreasing radial distance from the sun and the apparent proportionality to f_p^- can be attributed to the density dependence of the Debye length, which gives $f_{max} \propto f_p^-$ if the electron temperature remains constant.

Another possible explanation of the $f_p^+ < f < f_p^-$ noise is that it is caused by electron plasma oscillations at $f \simeq f_p^-$ which are Doppler-shifted to lower frequencies ($\mathbf{K}$ vectors directed toward the sun). This alternative is considered unlikely because for a two-stream instability, such plasma oscillations could only be produced by electrons streaming toward the sun from a source beyond 1.0 AU, which seems very implausible. Other possible plasma wave modes involving $\mathbf{K}$ vectors perpendicular to $\mathbf{B}$, such as the electron Bernstein modes at $f \simeq n f_g^-$, appear to be ruled out because of the

electric field direction, which is parallel to $\mathbf{B}$ (see Figure 13).

Of the various possible explanations of the $f_p^+ < f < f_p^-$ noise we believe that the ion sound wave is the most likely mode which could be associated with this noise. If these waves are ion sound waves, then there remains the important question of how these waves are generated and what effect they may have on the macroscopic properties of the solar wind. Since these waves apparently occur over large regions of the solar wind and are not particularly associated with discontinuities or other small-scale features where large currents may be present, the best possibility for generating these waves appears to be the heat flux driven instability suggested by *Forslund* [1970]. Further detailed comparisons with the Helios plasma measurements are clearly needed to identify definitely the instability mechanism involved in the generation of these waves. Although the maximum intensity of $f_p^+ < f < f_p^-$ noise is relatively small, with energy density ratios of typically $\epsilon_0 E^2/2nkT \simeq 10^{-5}$, this turbulence may nevertheless play a significant role in controlling the electron energy distribution in the solar wind, since these waves are present a large fraction (30–50%) of the time.

After several years of investigation [see *Gurnett and Frank*, 1975] the Helios plasma wave measurements have now finally provided clear evidence that intense electron plasma oscillations do occur in association with type III radio events. Rough estimates by *Gurnett and Frank* [1975] using the theory of *Papadopoulos et al.* [1974] indicate that electron plasma oscillations with field strengths of the order of 10 mV m^{-1} are required to explain low-frequency type III radio bursts. Field strengths nearly this large (5.26 mV m^{-1}) have now been found in association with a type III burst. Although the electron plasma oscillation model originally proposed by *Ginzburg and Zheleznyakov* [1958] can now be considered confirmed, there are still many questions remaining concerning the exact mechanism by which the plasma oscillations are converted to radio emissions. The most significant question is still concerned with the electric field strength of the plasma oscillations required to explain the power flux of the type III radio emission. If field strengths this large are always required to produce a significant level of radio emission, then it is surprising that such events are not found more often considering the large size of the type III radio source and the extensive measurements available from the Imp spacecraft near the earth [*Gurnett and Frank*, 1975]. Considerable future work is still needed to evaluate the various mechanisms for converting the plasma oscillation energy to radio emissions and to investigate further and understand the spatial structure of the type III radio emission.

When the Helios electric field measurements are compared with the previous Pioneer 8 and 9 results, it is apparent that a significant difference exists in the electric field spectrums and intensities detected by these two spacecraft. Of the two primary types of plasma waves detected by Helios (the $f_p^+ < f < f_p^-$ noise and electron plasma oscillations) neither was detected by Pioneer 8 and 9. As can be seen by comparing the spectrums in Figures 12 and 15 with the instrument noise levels in Figure 4, the $f_p^+ < f < f_p^-$ noise normally occurs with intensities too small to be detected by Pioneer 8 and 9. Unusually intense electron plasma oscillations, such as those in Figures 20 and 21, could have been detected by Pioneer 8 and 9; however, such large intensities occur so seldom that it is not surprising that events of this type were not observed. Thus insofar as comparisons are possible, there is no disagreement with the Pioneer measurements concerning the primary types

of plasma waves detected by Helios 1. However, when the waves and intensities detected by Pioneer 8 and 9 are compared with Helios measurements, significant differences are evident. In describing the Pioneer 8 and 9 results, *Scarf et al.* [1968] and *Scarf and Siscoe* [1971] discuss the occurrence of narrow band electric fields (at 400 Hz) of 1–10 mV m^{-1} and corresponding broadband (equivalent 100-Hz sine wave) amplitudes as large as 20–50 mV m^{-1}. In comparison, the peak electric field intensities detected by Helios are seldom larger than 1 mV m^{-1} and are more typically a few hundred microvolts per meter. As was described by *Siscoe et al.* [1971], Pioneer detects two principal types of plasma waves in the solar wind: noise bursts, or spikes, with durations of less than approximately 10 s and persistent long-duration events lasting typically 1 day or more. The short-duration noise bursts are shown to be closely correlated with discontinuities (such as shocks) in the solar wind, and the long-duration events are correlated with density enhancements preceding high-speed streams. The spectrums of both types of noise consist primarily of an intense low-frequency component at frequencies of f < 400 Hz. The short-duration noise bursts have intensities as large as 10 mV m^{-1} (1.6 × 10^{-6} V^2 m^{-2} Hz^{-1}) at 400 Hz, and the long-duration events frequently have broadband (equivalent 100-Hz sine wave) amplitudes exceeding 20 mV m^{-1}. In comparison, Helios 1, which has a threshold sensitivity nearly 40 dB better than Pioneer 8 and 9 at 400 Hz (see Figure 4), seldom detects any waves at all in the low-frequency (f < 400 Hz) channels, and even in cases where waves can be detected (Figure 8), the intensities are very low, typically not more than 10–30 μV m^{-1} in the 311- and 562-Hz channels. Although it is very difficult to compare the Helios multichannel measurements with the Pioneer broadband measurements, which involve certain assumptions regarding the shape of the spectrum [*Scarf et al.*, 1973], broadband intensities computed from the Helios peak spectrums, as shown in Figure 12, typically give broadband fields (0.3–1 mV m^{-1}) which are much smaller than the broadband amplitudes (20–50 mV m^{-1}) from Pioneer 8 and 9.

At the present time the difference in the low-frequency electric field intensities and characteristics given by Helios and Pioneer is not understood. Comments on two of the factors which could affect the comparisons between these two spacecraft are summarized below.

Solar activity. Because the primary Helios mission is being conducted during solar minimum conditions, whereas the Pioneer 8 and 9 measurements were made during a more active period of the solar cycle (1968–1969), it is possible that changes in the solar activity could account for some of the differences in the electric field intensities observed by Pioneer and Helios. This explanation could be important for the spike-like bursts and associated disturbances observed by Pioneer in association with interplanetary shocks, since the occurrence of interplanetary shocks has been very low during the period of the Helios observations. Many of the events discussed by *Scarf et al.* [1973] are closely associated with interplanetary shocks and have no counterpart in the Helios data currently available. In a few cases, electric field spectrums qualitatively similar to the shock-associated spikes and long-duration events detected by Pioneer 8 and 9 have been detected by Imp 6 and 8; however, the intensities in these cases also appear to be significantly smaller than the intensities observed by Pioneer 8 and 9.

Wavelengths shorter than the antenna length. When the plasma density is sufficiently large ($n \gtrsim$ 70 cm^{-3} for $T_e \simeq$ 10^5 °K), it is possible for the minimum wavelength of plasma

waves in the solar wind, $\lambda_{\min} = 2\pi\lambda_D$, to be less than the length of the Helios 1 antenna. If wavelengths this short occur, then the electric field strengths are underestimated, possibly by a large factor if $\lambda \ll l_{\text{eff}}$. Two tests can be performed with the Helios data to verify that the wavelengths being detected are longer than the antenna length. First, if the wavelengths are longer than the antenna, then the spin modulation pattern should be that of a simple dipole with two nulls per rotation. As is evident in Figures 13 and 17, both the $f_p^+ < f < f_p^-$ noise and the electron plasma oscillations clearly satisfy this criterion. If $\lambda \ll l_{\text{eff}}$, then a much more complex spin modulation pattern should occur with several nulls per rotation. Second, if wavelengths of $\lambda \ll l_{\text{eff}}$ occur, then large Doppler shifts should be evident in the electric field spectrums (except for the unlikely case that K is exactly perpendicular to the solar wind velocity). For the Helios 1 antenna, with $l_{\text{eff}} = 8.0$ m, wavelengths this short would have Doppler shifts greater than 50 kHz if a solar wind speed of 400 km s^{-1} is assumed. Doppler shifts this large are never observed for the electron plasma oscillations detected by Helios, and only the very highest frequency components of the $f_p^+ < f < f_p^-$ noise (see Figure 12) could possibly be associated with Doppler shifts this large (if we assume that the noise consists of ion sound waves). It should be noted that the intense low-frequency (f < 400 Hz) noise detected by Pioneer cannot be attributed to wavelengths too short to be detected by Helios, since the Doppler shift for these waves is not more than a few hundred hertz, implying wavelengths of 10^3 m or more. We conclude that the occurrence of wavelengths shorter than the Helios antenna length cannot account for the difference between Pioneer and Helios electric field measurements.

REFERENCES

Baumback, M. M., W. S. Kurth, and D. A. Gurnett, Direction-finding measurements of type III radio bursts out of the ecliptic plane, *Solar Phys.*, in press, 1977.

Belcher, J. W., and L. Davis, Jr., Large-amplitude Alfvén waves in the interplanetary medium, 2, *J. Geophys. Res.*, *76*, 3534, 1971.

Benediktov, E. A., G. G. Getmantsev, N. A. Mityakov, V. O. Rapoport, and A. F. Tarasov, Relation between geomagnetic activity and the sporadic radio emission recorded by the electron satellites, *Kosm. Issled.*, *6*, 946, 1968.

Buneman, O., Instability, turbulence and conductivity in a current-carrying plasma, *Phys. Rev. Lett.*, *1*, 8, 1958.

Burlaga, L. F., Hydromagnetic waves and discontinuities in the solar wind, *Space Sci. Rev.*, *12*, 600, 1971.

Coleman, P. J., Jr., Hydromagnetic waves in the interplanetary plasma, *Phys. Rev. Lett.*, *17*, 207, 1966.

Fainberg, J., L. G. Evans, and R. G. Stone, Radio tracking of solar energetic particles through interplanetary space, *Science, 178*, 743, 1972.

Forslund, D. W., Instabilities associated with heat conduction in the solar wind and their consequences, *J. Geophys. Res.*, *75*, 17, 1970.

Fredricks, R. W., Electrostatic heating of solar wind ions beyond 0.1 AU, *J. Geophys. Res.*, *74*, 2919, 1969.

Ginzburg, V. L., and V. V. Zheleznyakov, On the possible mechanism of sporadic radio emission (radiation in an isotropic plasma), *Sov. Astron. A. J.*, *2*, 653, 1958.

Gurnett, D. A., The earth as a radio source: Terrestrial kilometric radiation, *J. Geophys. Res., 79,* 4227, 1974.

Gurnett, D. A., and L. A. Frank, The relationship of electron plasma oscillations to type III radio emissions and low-energy solar electrons, *Solar Phys., 45,* 477, 1975.

Haddock, F. T., and H. Alvarez, The prevalence of second harmonic radiation in type III bursts observed at kilometric wavelengths, * *Solar Phys., 29,* 183, 1973.

Hartle, R. E., and P. A. Sturrock, Two-fluid model of the solar wind, *Astrophys. J., 151,* 1155, 1968.

Hatch, A. J., and H. B. Williams, The secondary electron resonance mechanism of low-pressure high-frequency gas breakdown, *J. Appl. Phys., 25,* 417, 1954.

Hatch, A. J., and H. B. Williams, Multipacting modes of high frequency gaseous breakdown, *Phys. Rev., 112,* 681, 1958.

Hollweg, J. V., Waves and instabilities in the solar wind, *Rev. Geophys. Space Phys., 13,* 263, 1975.

Kaiser, M. L., The solar elongation distribution of low-frequency radio bursts, *Solar Phys., 45,* 181, 1975.

Kurth, W. S., M. M. Baumback, and D. A. Gurnett, Direction-finding measurements of auroral kilometric radiation, *J. Geophys. Res., 80,* 2764, 1975.

Papadopoulos, K., M. L. Goldstein, and R. A. Smith, Stabilization of electron streams in type III solar radio bursts, *Astrophys. J., 190,* 175, 1974.

Parker, E. N., Dynamics of the interplanetary gas and magnetic fields, *Astrophys. J., 128,* 664, 1958.

Rodriguez, P., and D. A. Gurnett, Electrostatic and electromagnetic turbulence associated with the earth's bow shock, *J. Geophys. Res., 80,* 19, 1975.

Scarf, F. L., and G. L. Siscoe, The Pioneer 9 electric field experiment, 2, Observations between 0.75 and 1.0 AU, *Cosmic Electrodynamics, 2,* 44, 1971.

Scarf, F. L., G. M. Crook, I. M. Green, and P. F. Virobik, Initial results of the Pioneer 8 VLF electric field experiment, *J. Geophys. Res., 73,* 6665, 1968.

Scarf, F. L., R. W. Fredricks, L. A. Frank, and M. Neugebauer, Nonthermal electrons and high-frequency waves in the upstream solar wind, 1, Observations, *J. Geophys. Res., 76,* 5162, 1971.

Scarf, F. L., R. W. Fredricks, and I. M. Green, Comparison of deep space and near-earth observations of plasma turbulence at solar wind discontinuities, Solar Wind, *NASA Spec. Publ. 308,* 421, 1972.

Scarf, F. L., I. M. Green, and J. S. Burgess, The Pioneer 9 electric field experiment, 3, Radial gradients and storm observations, *Astrophys. Space Sci., 20,* 499, 1973.

Schulz, M., and A. Eviatar, Electron temperature asymmetry and the structure of the solar wind, *Cosmic Electrodynamics, 2,* 402, 1972.

Siscoe, G. L., F. L. Scarf, I. M. Green, J. H. Binsack, and H. S. Bridge, Very low frequency electric fields in the interplanetary medium: Pioneer 8, *J. Geophys. Res., 76,* 828, 1971.

Slysh, V. I., The measurement of cosmic radio emission at 210 and 2200 kilocycles per second to eight earth radii on the automatic interplanetary station Zond-2, *Kosm. Issled., 3,* 760, 1965.

Smith, D. F., Type III radio bursts and their interpretation, *Space Sci. Rev., 16,* 91, 1974.

Stix, T., *The Theory of Plasma Waves,* p. 32, McGraw-Hill, New York, 1962.

Sturrock, P. A., Spectral characteristics of type III solar radio bursts, *Nature, 192,* 58, 1961.

Tidman, D. A., T. J. Birmingham, and H. M. Stainer, Line splitting of plasma radiation and solar radio outbursts, *Astrophys. J., 146,* 207, 1966.